University of Crete, Physics Department and FORTH, IESL
Microelectronics Research Group (MRG)
Heraklion, Crete, Greece

Molecular beam epitaxy of III-V semiconductors in Greece: From III-Arsenides to III-Nitrides

Alexandros Georgakilas

37th Panhellenic conference on Solid-State Physics and Materials Science

17-20 September, 2023, Thessaloniki

Outline

- **History of MBE in Greece**
- **Introduction for III-V Semiconductors and Molecular Beam Epitaxy**
- **Research on GaAs and related arsenide-compounds (III-As)**
- **Research on GaN and related nitride-compounds (III-N)**
- **Conclusions**
- **Acknowledgements**

III-V Molecular Beam Epitaxy in Crete

- **Prof. Aris Christou has been associated with University of Crete and/or Research Center of Crete (now FORTH) from mid 80s till early 90s**
  - ***In 1985, a VG 80H Molecular Beam Epitaxy (MBE) system for III-As MBE was installed***
  - ***4-5 years later, a VG 80V MBE chamber for Si and Ge MBE was added***
- **In 1997-1998, a RIBER 32P system for III-Nitrides MBE was purchased and installed under my coordination**
- **Constant philosophy of MBE research has been to go beyond studies of growth and surface-science physics by making available novel heterostructure materials for physics and device engineering research**
  - **Material available to all researchers of the Microelectronics Research Group (MRG) of FORTH and Univ. Crete**

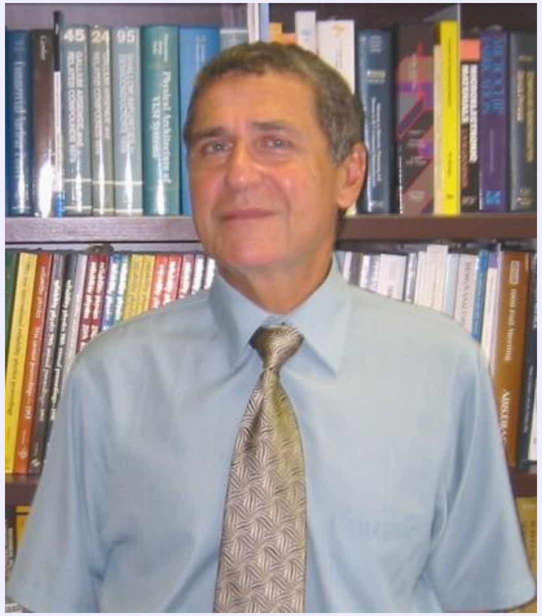

Prof. Aris Christou

Professor at Univ. Maryland

Department of Materials Science and Engineering

Department of Mechanical Engineering

2012 Micro & Nano Award

III-V MBE history

UoC & FORTH

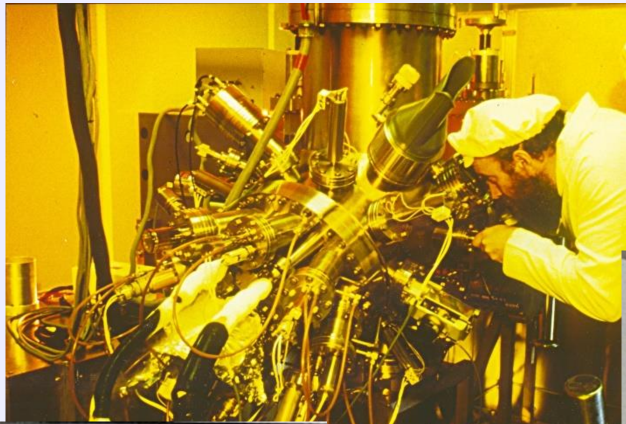

1985 at Knossos

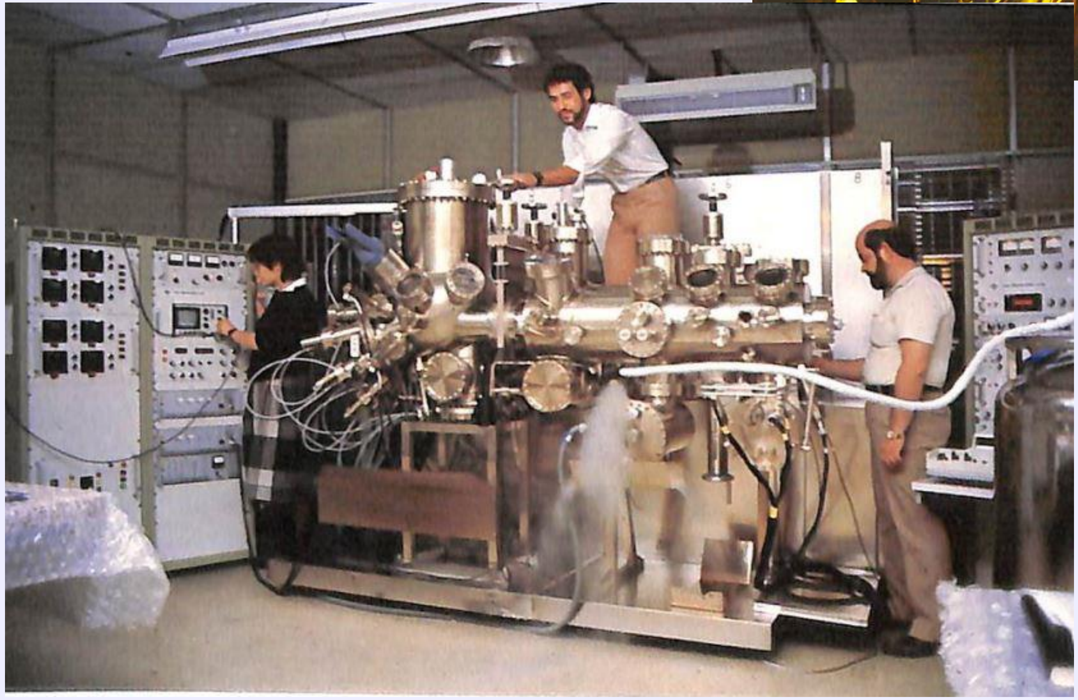

2004 at Voutes

III-V semiconductors

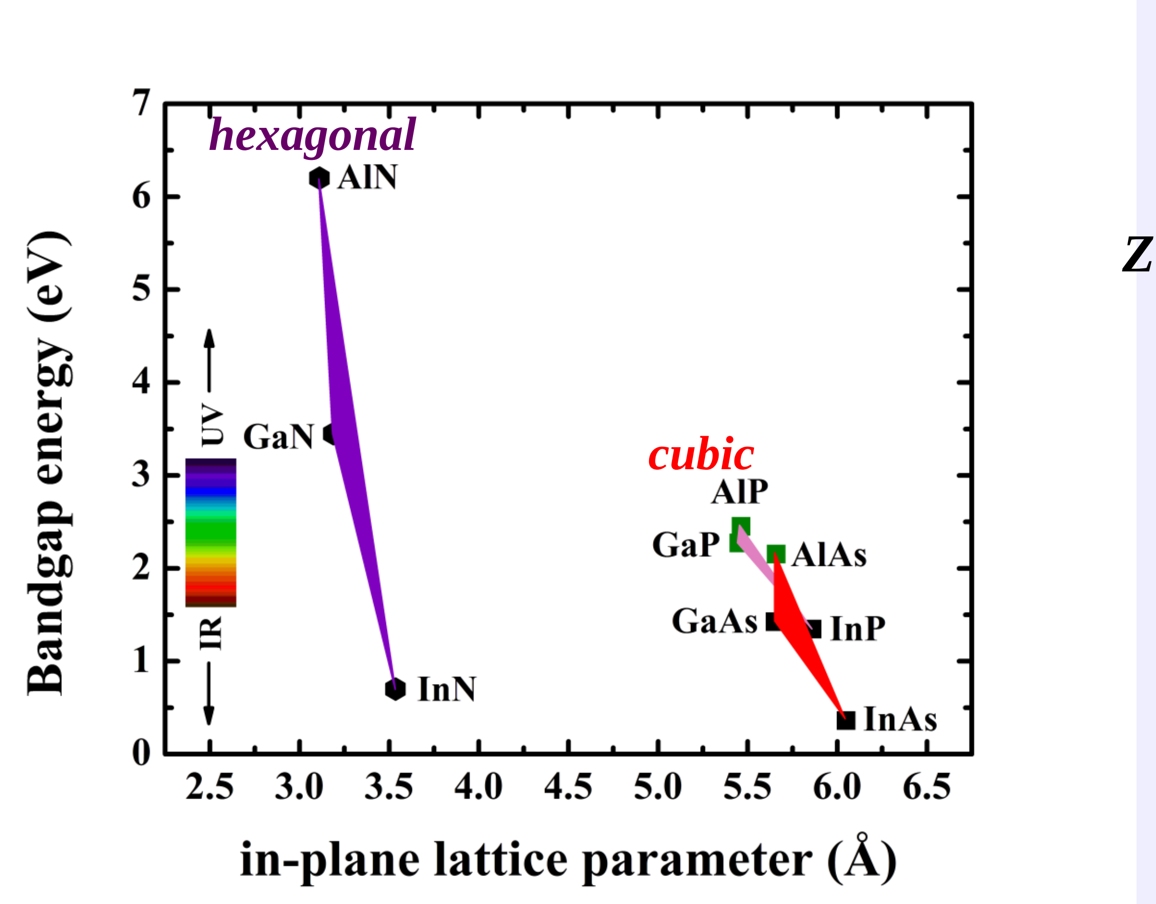

Cubic
Zinc blende / Sphalerite

GaAs, InP, InSb

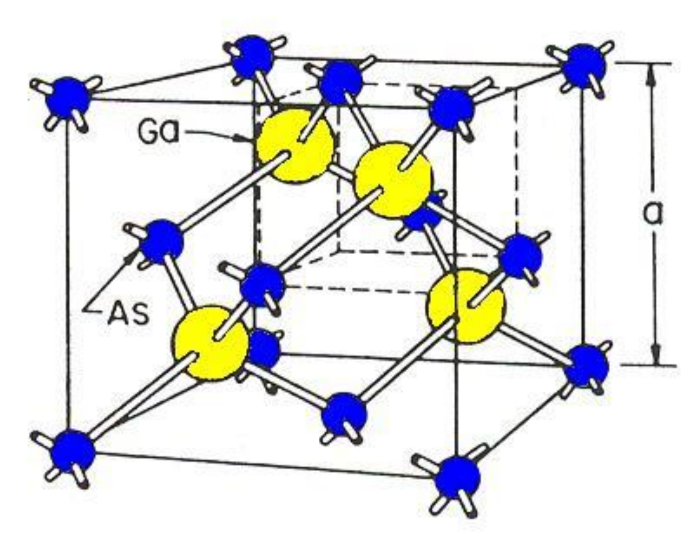

Hexagonal
Wurtzite

GaN, AlN, InN

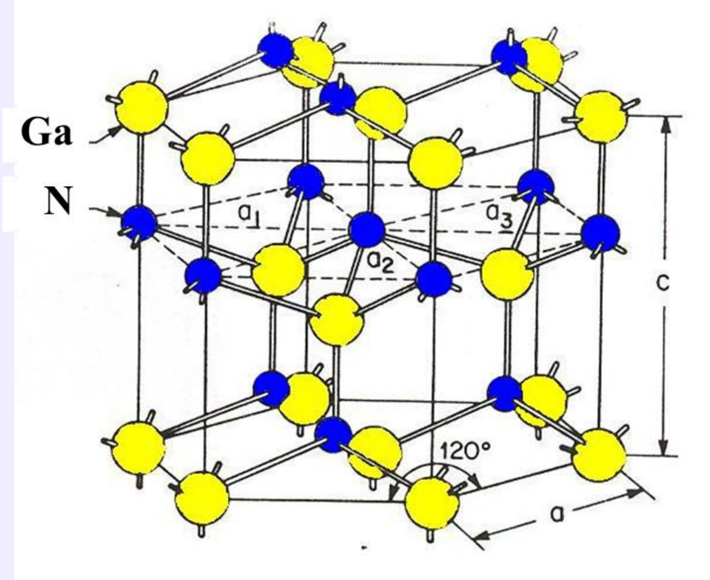

Basic concepts & experimental configuration

Epitaxy

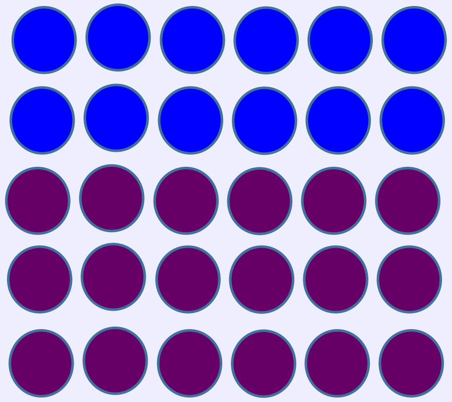

Crystalline epilayer

Crystalline substrate

T_{sub} near the highest possible prior to material decomposition, and allowing sufficient residence time of adatoms on the surface

Molecular Beam Epitaxy

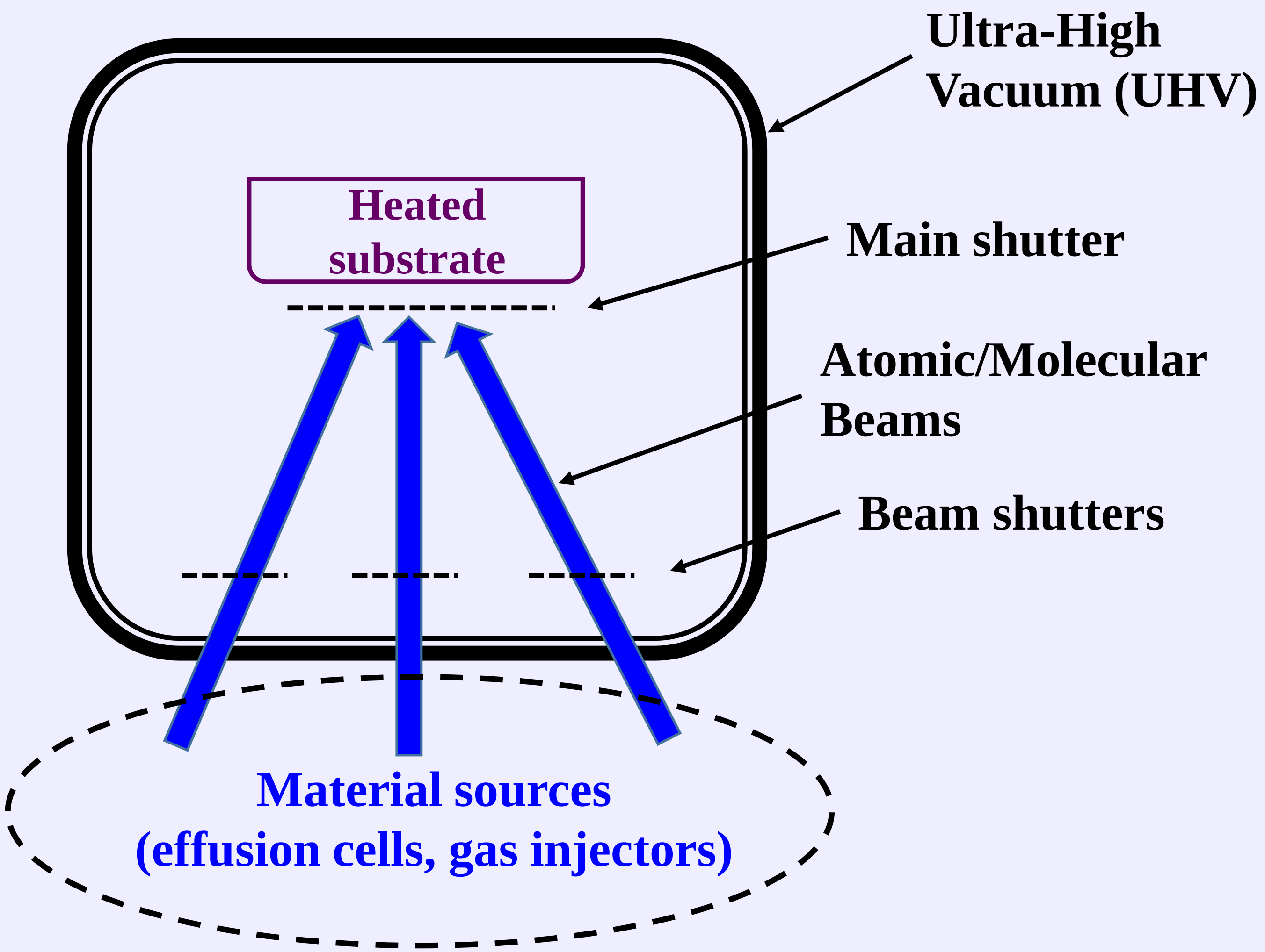

Ultra-High Vacuum (UHV)

Heated substrate

Main shutter

Atomic/Molecular Beams

Beam shutters

Material sources (effusion cells, gas injectors)

MBE of III-Arsenides / III-Nitrides

UoC & FORTH

Solid-source for Arsenic
Knudsen cell

MBE / Solid-source MBE

As$_4$ molecules are evaporated from solid As heated in the PBN crucible

→ Beam of As$_4$ molecules

Ga Atomic Beam from a Knudsen cell

Gas-source for Nitrogen
RF plasma source

Plasma-source MBE (PAMBE)

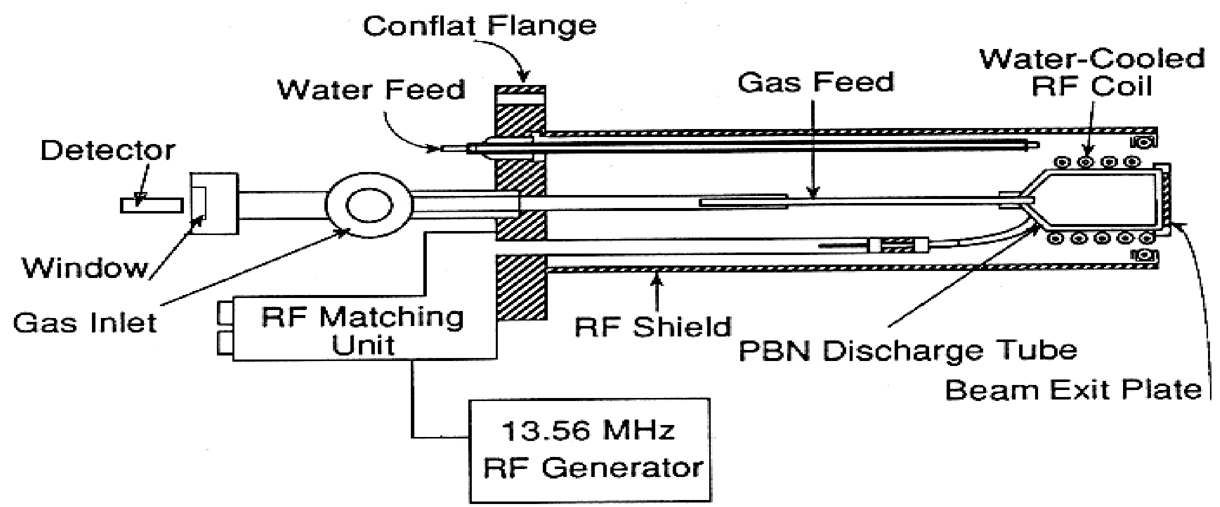

RF-power induced plasma is generated for the injected molecular N$_2$ gas in a PBN tube

→ Beam of reactive N$_2$* and N species

Mainly excited molecular species: *E. Iliopoulos et al., J. Cryst. Growth 278, 426 (2005)*

GaAs MBE

Ga(Al,In)As MBE is carried out under As-stabilized surface conditions → c (2x8) surface reconstruction for (001) GaAs surface

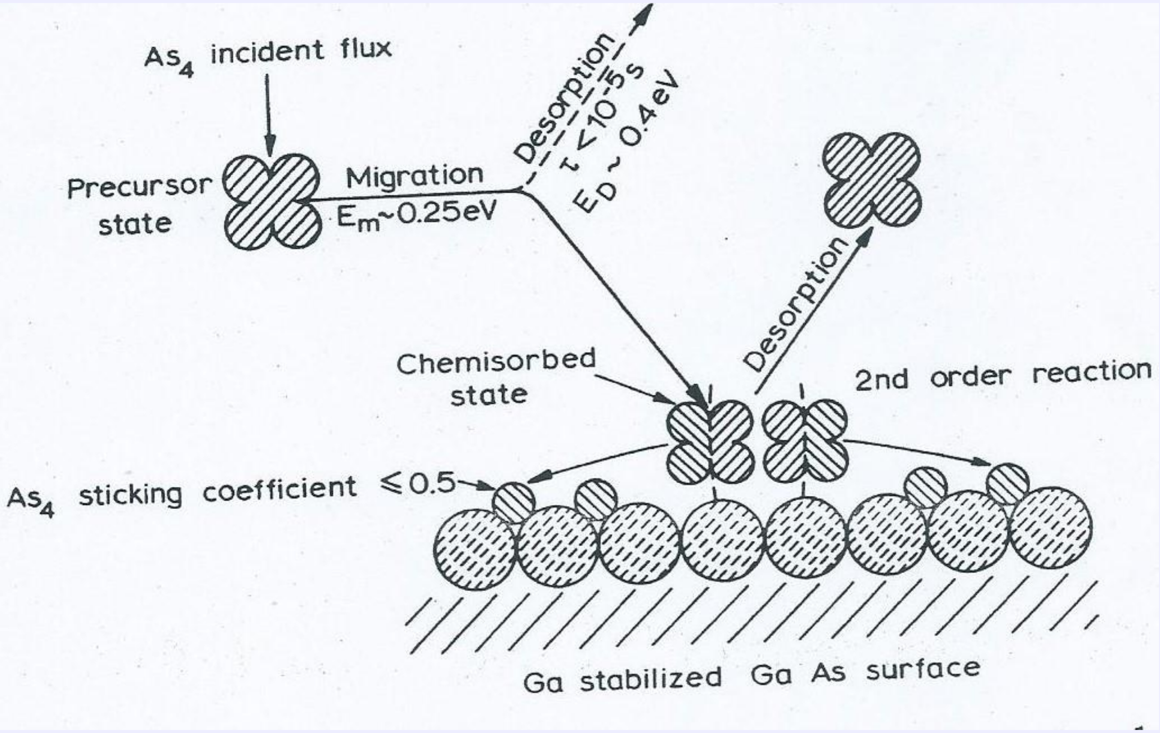

From B. A. Joyce, Chapter 3 in "Molecular Beam Epitaxy and Heterostructures", eds. L.L. Chang and K. Ploog, NATO ASI Series E, no. 87

As atoms do not stick on the surface without presence of Ga atoms for bonding

Pairs of As_4 molecules react on adjacent Ga sites → 2 As atoms/pair are incorporated into the solid and an As_4 molecule is desorbed from the surface

⇒ Maximum sticking coefficient of As_4 is 0.5

Excess As is not incorporated → stoichiometric GaAs growth

GaAs decomposes at lower T_{sub} than Ga desorption

Ga droplets form from excess Ga on the surface

Typical use of $F_{As4} \sim 4\,F_{Ga}$

GaN PAMBE

Ga(Al,In)N (0001) PAMBE is carried out under III metal-stabilized surface conditions

A **Ga bilayer** is stable on the (0001) GaN surface under Ga-rich growth conditions. High mobility of Ga adatoms in this adlayer

Northrup et al, PRB 61, 9932 (2000)

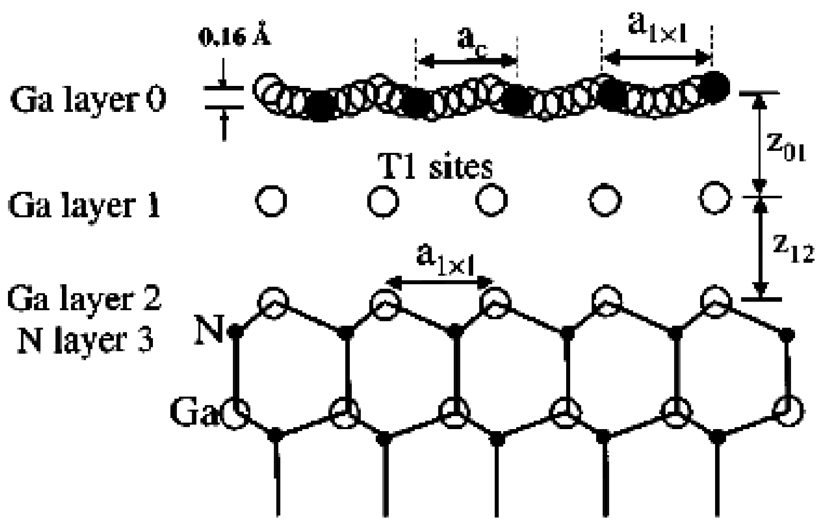

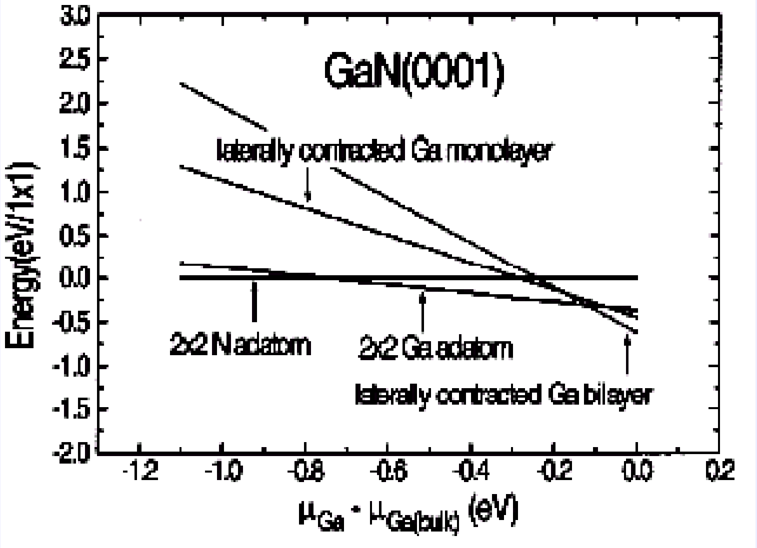

Metallic adlayers are favorable on all III-Nitride (0001) surfaces under metal-rich growth conditions

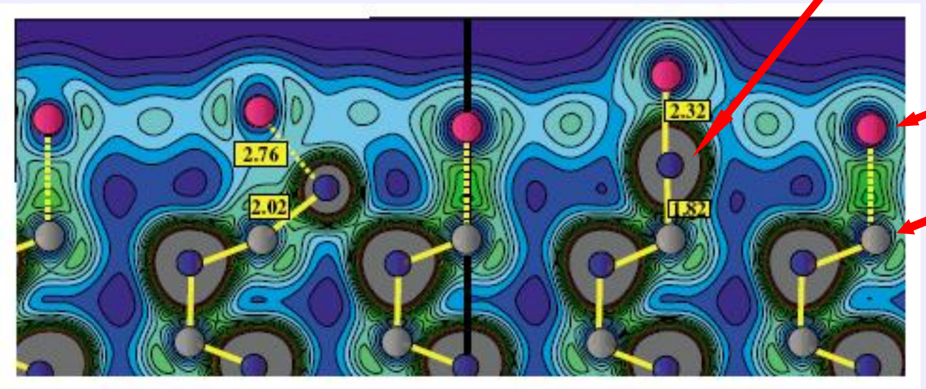

N adatom

In adlayer

Ga

Low diffusion barrier for N adatoms below a metallic adlayer

Neugebauer et al, PRL 90, 056101 (2003)

Important differences in GaN and InN PAMBE

MBE is carried out at T_{sub} prior to the initiation of decomposition

GaN (0001) is grown under Ga-rich conditions: Ga-Flux / N-flux >> 1.0, e.g. 1.6

Excess Ga atoms are desorbed from the surface – dynamically stable Ga bilayer

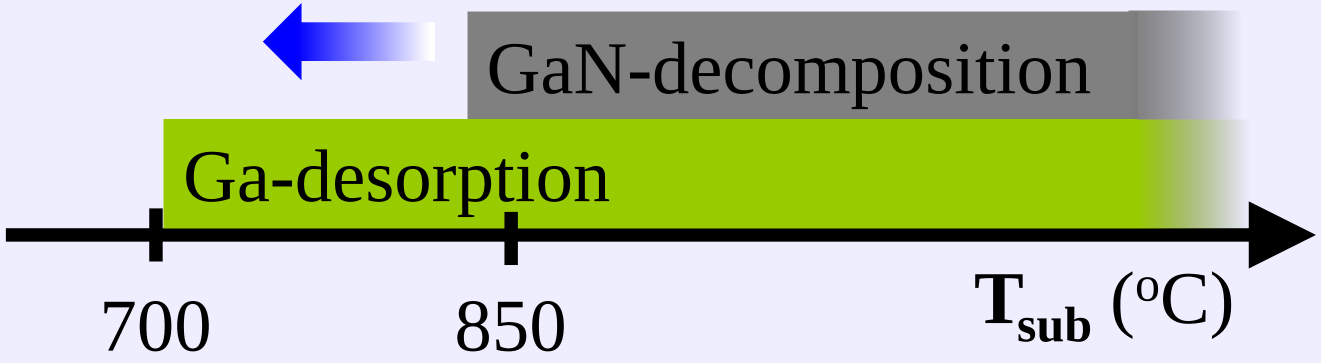

GaN-decomposition

Ga-desorption

700

850

T_{sub} (^{o}C)

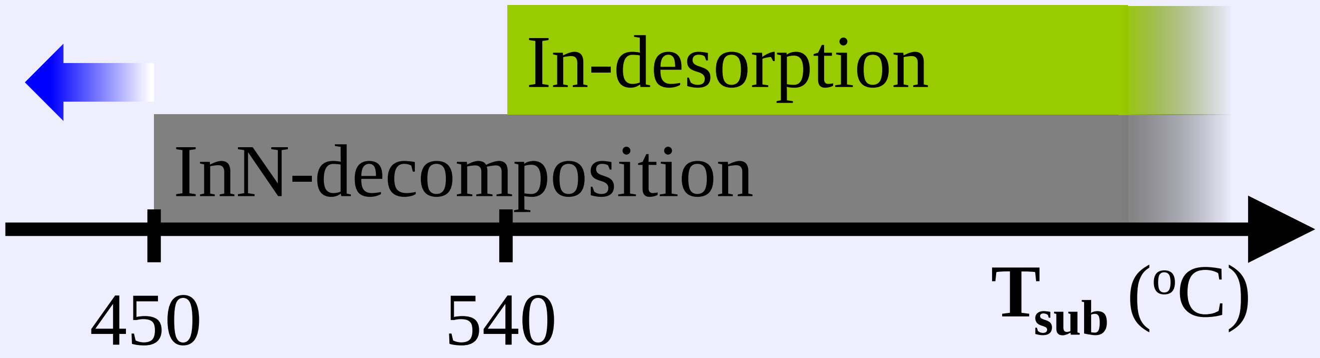

In-desorption

InN-decomposition

450

540

T_{sub} (^{o}C)

InN (0001) cannot be grown under In-rich conditions

Excess In atoms form In droplets on the surface

⇒ Ga-Flux / N-flux ≈ 1.0+ and growth interruption for nitridation

Considerations for Homoepitaxy

Growth mode and "quality" of epitaxy depend on the diffusion length λ_S of adatoms on the surface, before they are incorporated into the solid

Main effect from T_{sub}. Additional influence from surface structure/composition, substrate miscut angle (mean distance of surface steps) and rate of deposition (time to complete 1ML)

$\lambda_S = \sqrt{D_S \tau_S}$ **with** $D_S \sim e^{-\Delta G_S/kT_{sub}}$ **and** τ_S**: time for incorporation into the solid (for ~ 1ML deposition)**

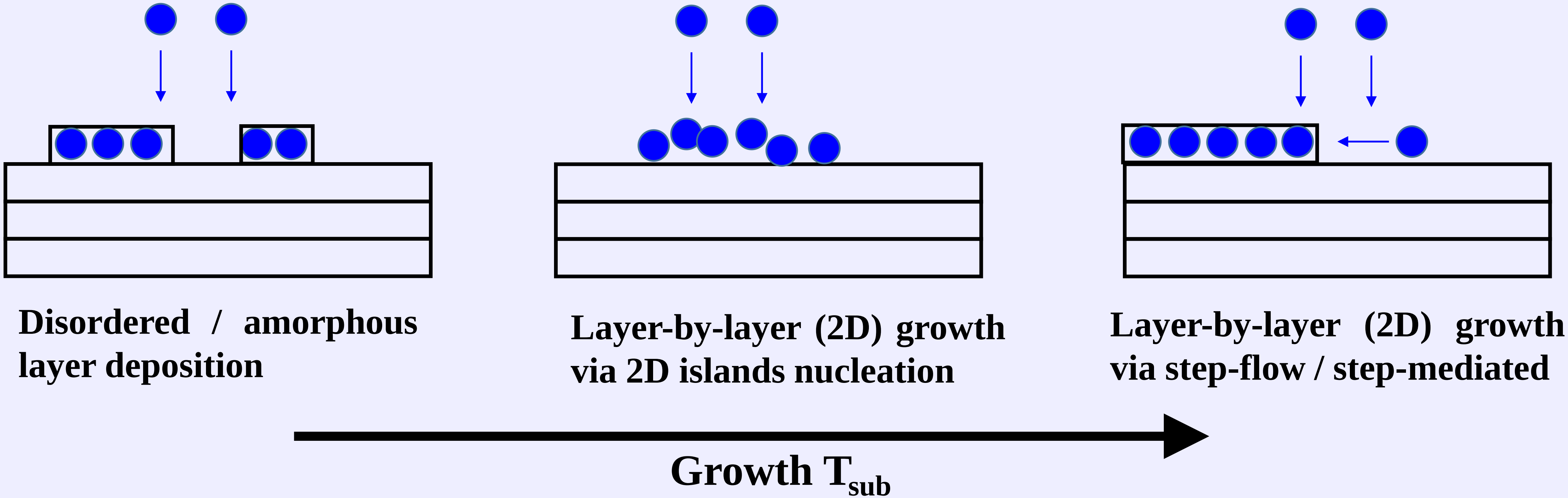

Disordered / amorphous layer deposition

Layer-by-layer (2D) growth via 2D islands nucleation

Layer-by-layer (2D) growth via step-flow / step-mediated

Growth T_{sub}

Considerations for Heteroepitaxy

Heteroepitaxy → Epilayer and substrate are different crystalline materials

Assuming chemical bonding is possible between substrate’s and epilayer’s atoms, main question is how well the epilayer’s crystal could be accommodated on the substrate’s crystal

Compatible crystal spacing ? ***Compatible crystal symmetry ?***

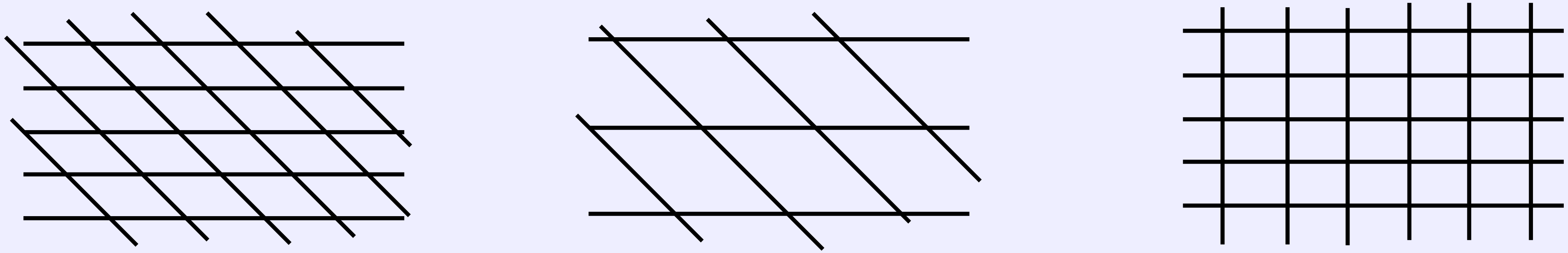

Misfit *f* between substrate and epilayer (along a direction on the surface)

$$f = \frac{|a_s - a_f|}{a_f}$$

Strain ε

$$\varepsilon = \frac{a_{strained} - a_{unstrained}}{a_{unstrained}}$$

Strain *Energy/area for epilayer thickness h*

$$E_\varepsilon = \varepsilon^2 Bh$$

$$B = 2\mu_f \frac{(1+\nu)}{(1-\nu)}$$ in elastically isotropic solid

Misfit strain relaxation

Formation of 3D islands

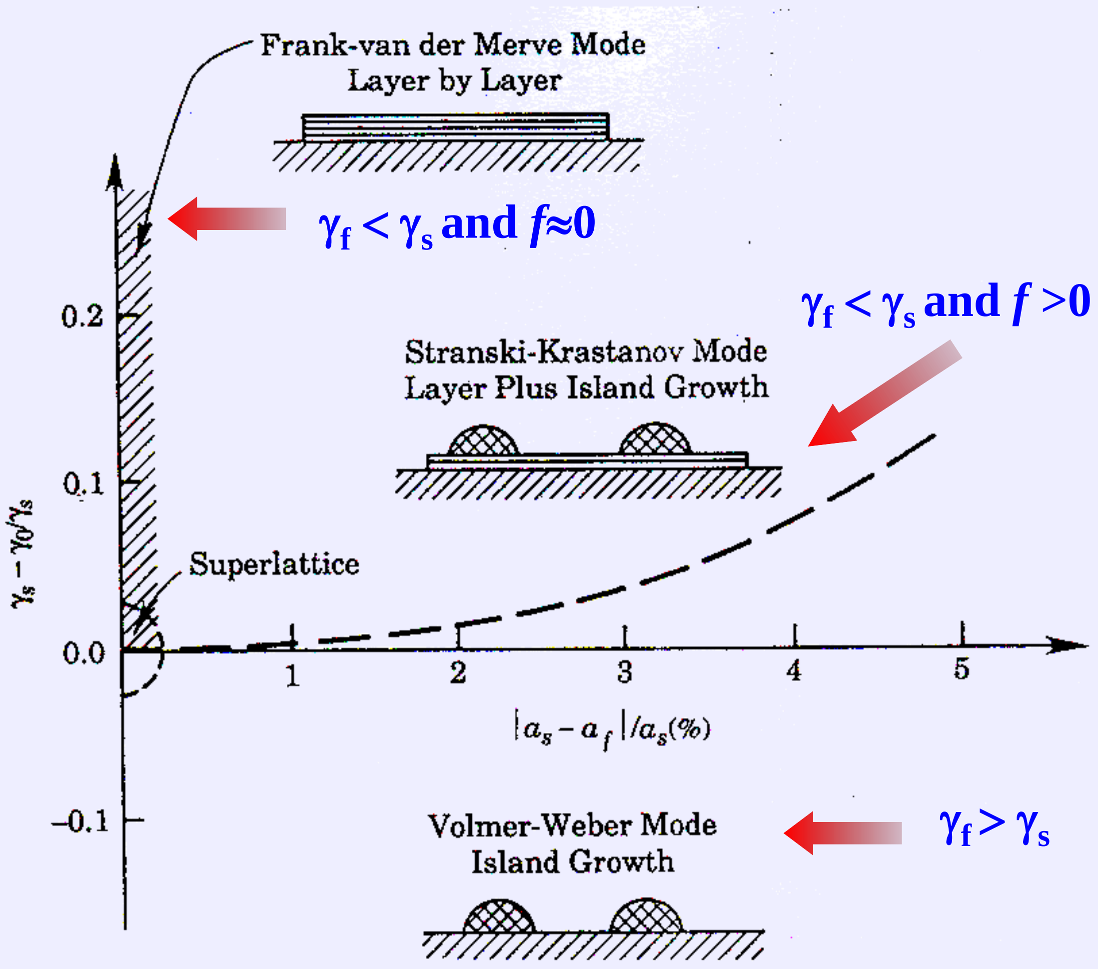

$\gamma_f < \gamma_s$ **and** $f \approx 0$

$\gamma_f < \gamma_s$ **and** $f > 0$

$\gamma_f > \gamma_s$

From "Electronic Thin Film Science: For Electrical Engineers and Materials Scientists", K.-N. Tu, J. W. Mayer and L. C. Feldman Macmillan, 1992, Chapter 7 (adapted from M. H. Grabow and G. H. Gilmer, 1986)

Formation of misfit dislocations at the epilayer/substrate interface

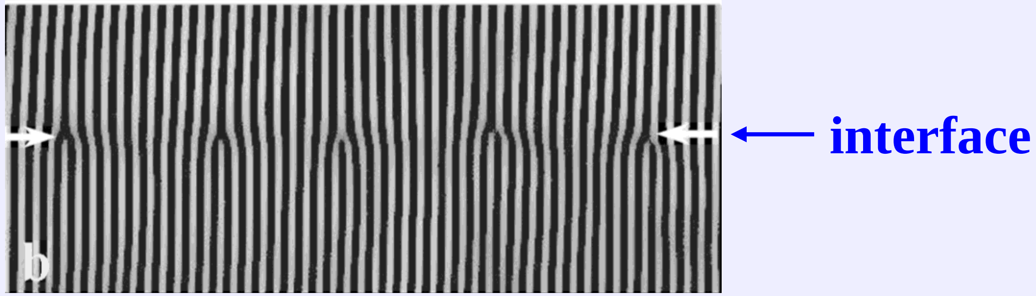

From E. Dimakis et al, J. Appl. Phys. 97, 113520 (2005)

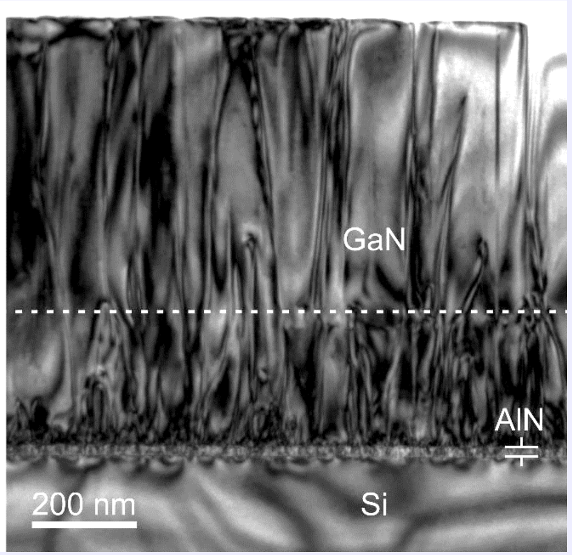

Threading dislocations **result as a side-effect of strain relaxation by misfit dislocations and 3D growth mode**

Why MBE of heterostructure materials

I. *Band gap engineering for optimum device active regions*

- **No defects are allowed at these hetero-interfaces**

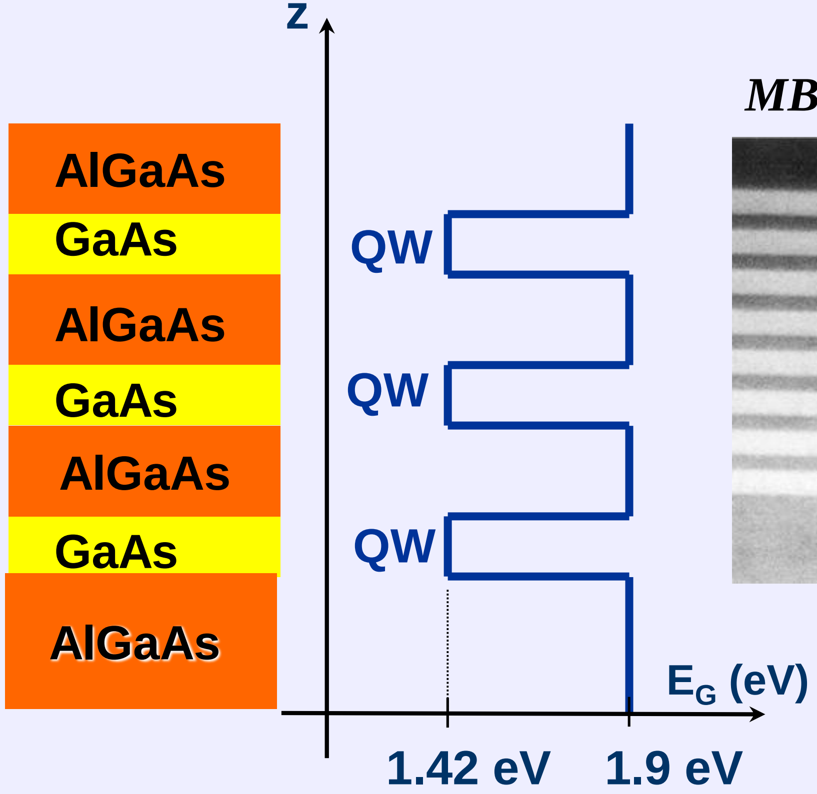

MBE AlGaAs/GaAs QWs

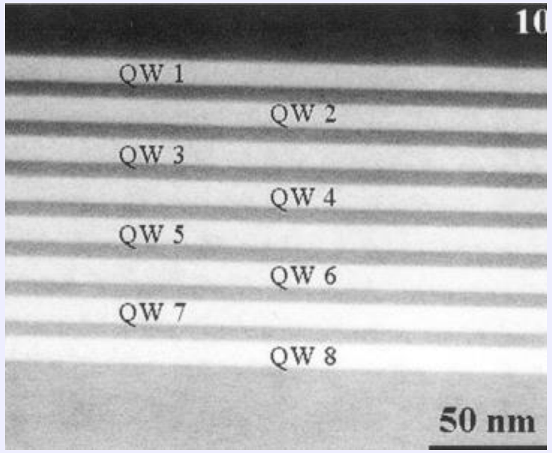

II. ***Heteroepitaxial structures for***

(a) combination-integration of different substrate and epi materials and corresponding device functions

(b) substitution of non-existing substrates

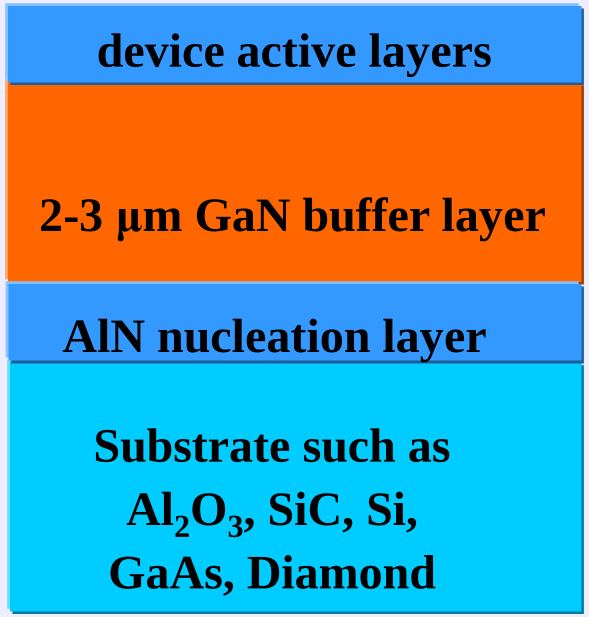

device active layers

2-3 μm GaN buffer layer

AlN nucleation layer

Substrate such as Al_2O_3, SiC, Si, GaAs, Diamond

III-Arsenide Semiconductors

InAlAs/InGaAs HEMT material on InP (001)

- $In_{0.52}Al_{0.48}As$ ($E_G \approx 1.44$ eV) and $In_{0.53}Ga_{0.47}As$ ($E_G \approx 0.75$ eV) comprise an important heterostructure material system for both optoelectronics and ultra-high frequency nanoelectronics
  - ➢ HEMTs with Lg=25nm have exhibited F_T and F_{max} above 700 GHz

    H.-B. Jo et al, Appl. Phys. Express 12, 054006 (2019)
  - ➢ Light Emitting Devices with $In_{0.53}Ga_{0.47}As$ ($E_G \approx 0.75$ eV) QWs operate at the desirable wavelength of 1.55 μm for optical fiber data transmission

- InAlAs, InGaAs alloys do not exist as substrates but $In_{0.52}Al_{0.48}As$ and $In_{0.53}Ga_{0.47}As$ are lattice matched with InP

- 3 decades ago, we developed MBE know-how for state-of-the-art $In_{0.52}Al_{0.48}As/In_{0.53}Ga_{0.47}As$ HEMT material on InP (001) substrates, by addressing the following critical issues
  - ➢ Preparation of the InP (001) surface prior to $In_{0.52}Al_{0.48}As$ buffer layer growth

    F. Peiro et al, J. Vac. Sci. Technol. B10, 2148 (1992)
  - ➢ Optimization of $In_{0.52}Al_{0.48}As$ buffer growth, concerning its structural and electronic properties

    A. Georgakilas et al, J. Electroch. Soc. 140, pp. 1503-1509 (1993)

InP (001) substrate surface preparation

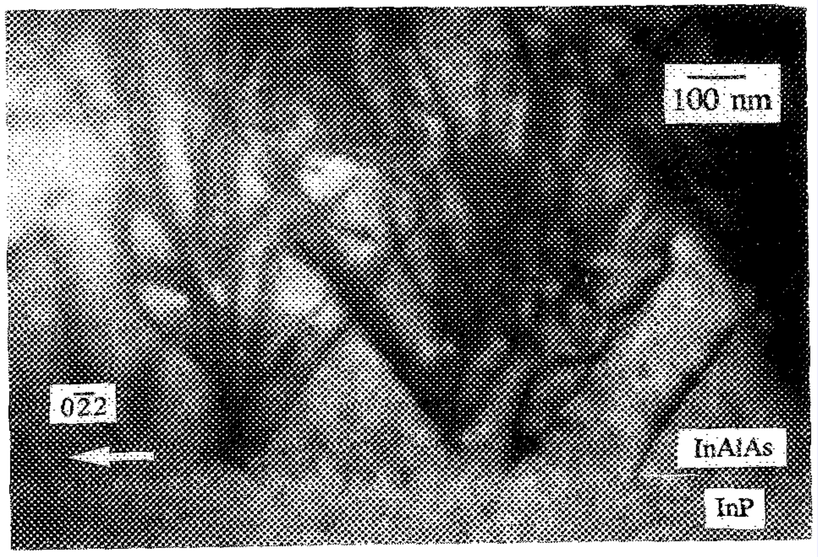

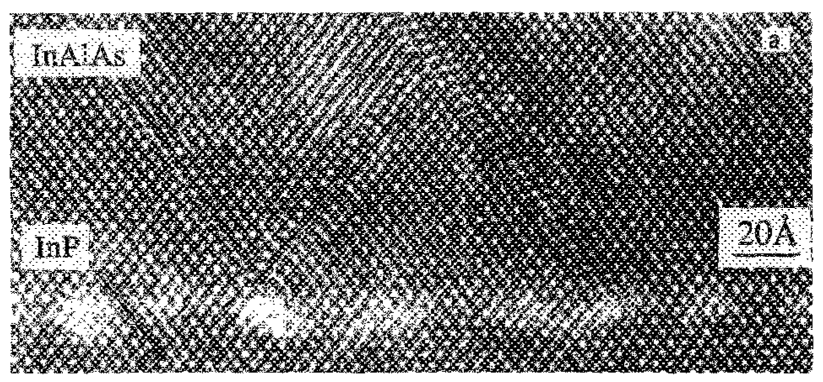

- **InP oxide desorption and preparation of an atomically smooth and clean surface in a III-Arsenides MBE system (without P beam) is very challenging**
  - ***roughening, P atoms sublimation and exchange with As atoms → formation of strained InAs interlayer***

- **Standard oxide desorption was at $T_{sub} \approx 500°$, with 2x1 RHEED pattern observation for the InP:As surface**

✓ **We adopted oxide desorption without As-flux up to T_{sub}~ 530°C, corresponding to RHEED pattern transition from 2x1 to 4x2 (In-rich) – then instantaneously As_4 beam is incident and $In_{0.52}Al_{0.48}As$ growth starts**

F. Peiro et al, J. Vac. Sci. Technol. B10, 2148 (1992)

A. Georgakilas et al, J. Electroch. Soc. 140, 1503 (1993)

State-of-the-art InAlAs/InGaAs HEMT material

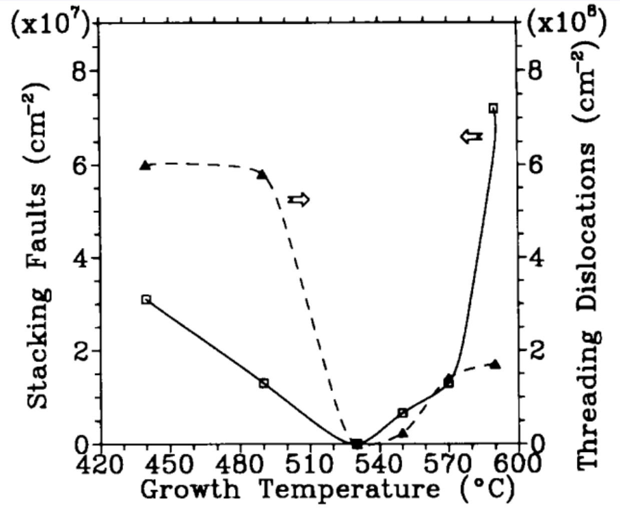

- ➢ Growth of thick $In_{0.52}Al_{0.48}As$ buffer layer is difficult
  - ➢ Strong Al-As bonds, weak In-As bonds
  - ➢ Crystal defects at low T_{sub}, compositional modulations and crystal defects at high T_{sub}
- ✓ Short T_{sub} window at ~530°C that can be detemined by the 2x1 to 4x2 RHEED pattern transition on the InP surface
- ✓ $In_{0.60}Ga_{0.40}As$-channel HEMTs without trap-related "kink-effect" in I-V characteristics, g_m= 530 mS/mm for Lg=1.3µm, Wg= 180 µm

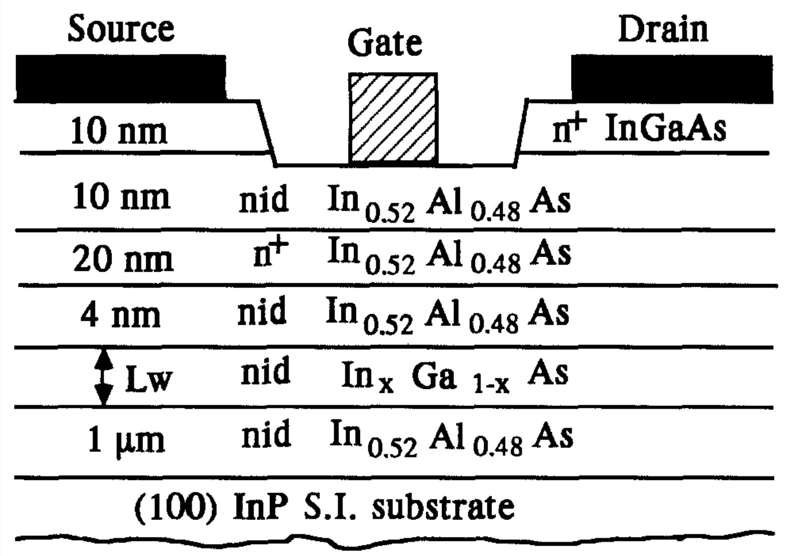

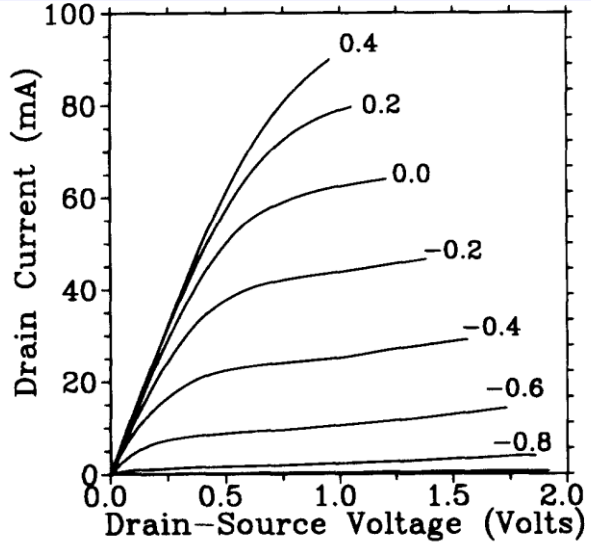

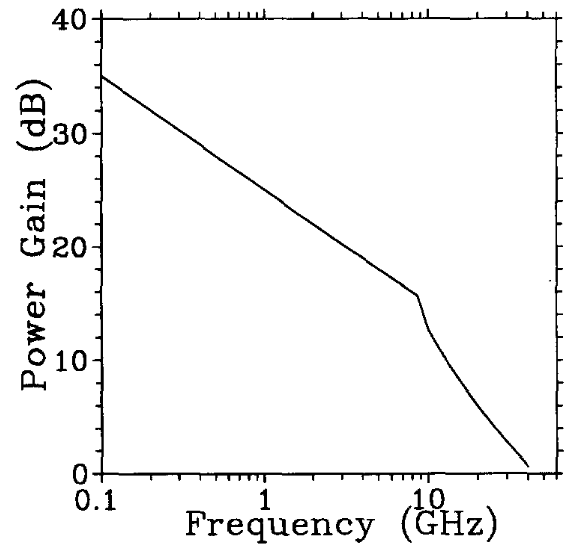

A. Georgakilas et al, J. Electroch. Soc. 140, 1503 (1993)

InAlAs compositional modulation effects

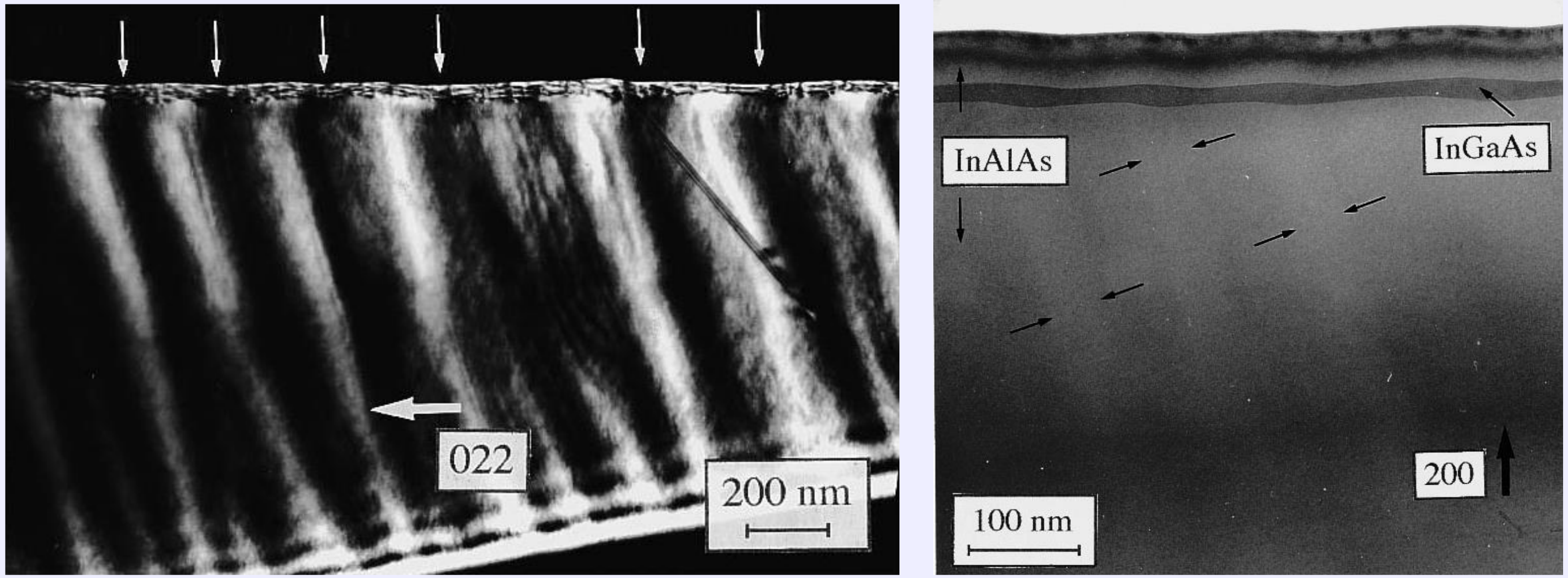

F. Peiro et al, Appl. Phys. Lett. 66, 2391 (1995)

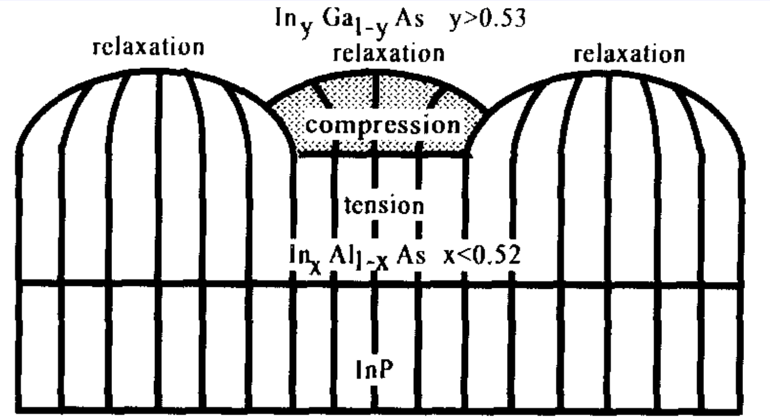

Figure 4. Model for the direct growth of InGaAs quantum wires on tensile InAlAs buffer layers.

A. Georgakilas et al, Microel. Eng. 41/42, 583 (1998)

- **InAlAs develops compositional modulations at high T_{sub}**
- ✓ **We showed that the asymmetric array of steps on the surface of InP (001) misoriented by 4° off toward [110] triggers a unidirectional modulation of InAlAs composition and surface undulation**
- ✓ **An overgrown InGaAs QW exhibits thickness modulation → potentially exploitable for QWires formation**

GaAs/AlGaAs Heterostructures for Optoelectronics

- **In 1998, a hardcore European project in GaAs optoelectronics started, requiring the development of MBE material and fabrication of GaAs heterostructure Laser Diodes in Crete**

ESPRIT 28998, BONTEC: *"Bonding Technology for Monolithic Integration of GaAs Optoelectronic Devices on Si Substrates for chip-to-chip Optical Interconnections"* (1/9/1998-31/12/2000)

We worked in collaboration with Institute of Microelectronics, NCSR Demokritos and Max Planck Institute of Microstructure Physics, Halle, Germany on a Greek idea for GaAs-based Optical Interconnects on Si CMOS circuits:

***Patent GR1003602 (19/06/2001): "Procedure for the wafer scale integration of gallium arsenide based optoelectronic devices with silicon based integrated circuits"* (and EP1130647 application)**
George Halkias, Dimitrios Tsoukalas, Alexandros Georgakilas

- ✓ **Extremely challenging/intensive work to catch up with over 2 decades of worldwide developments in physics and engineering of GaAs heterostructure Laser Diodes, Waveguides and Photodetectors**

- ✓ **Established the foundations for continuation of more elaborate optoelectronics research by newly recruited researchers/professors in Crete**

THE BONTEC APPROACH FOR OPTICAL INTERCONNECTS

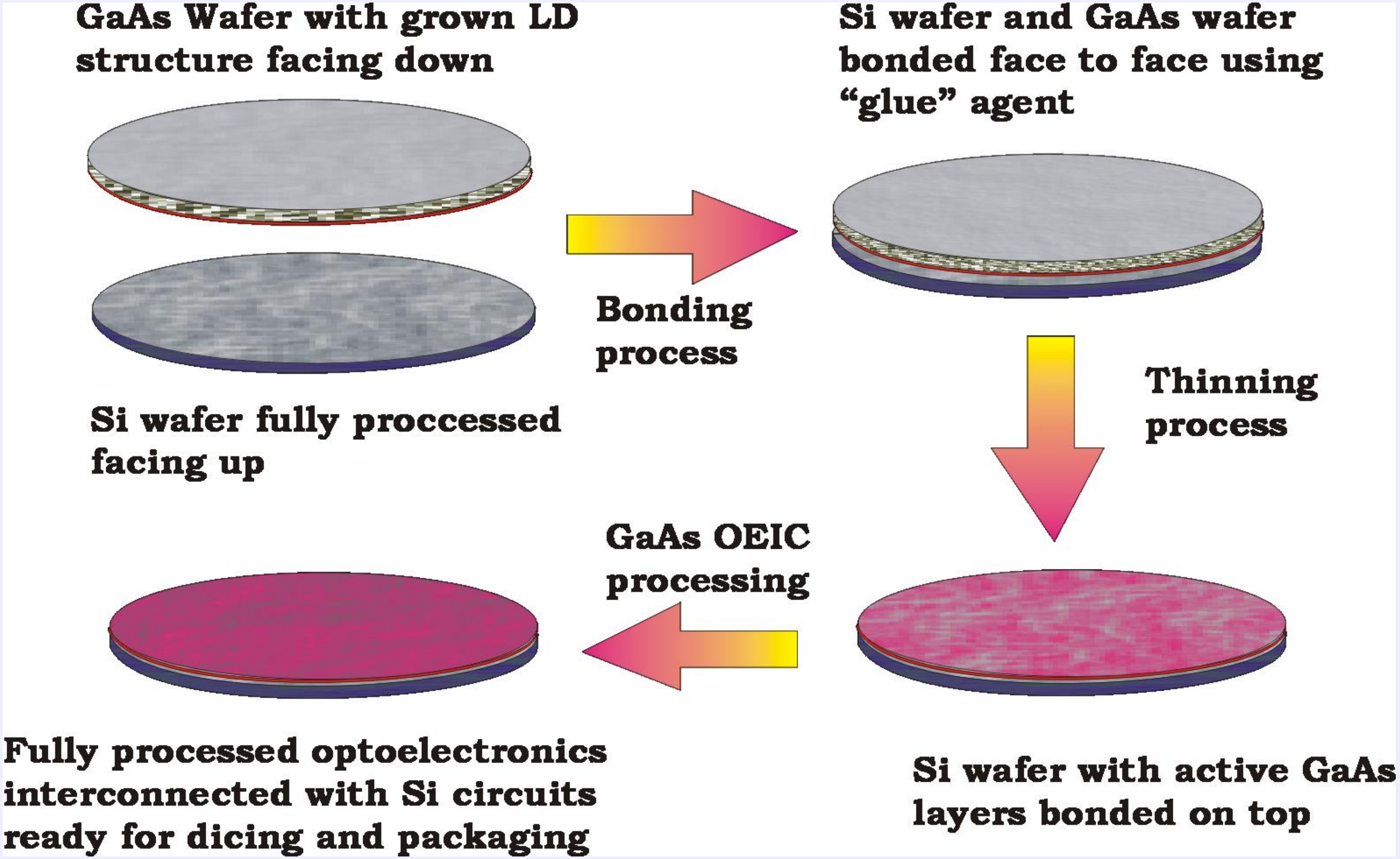
GaAs Wafer with grown LD structure facing down

Si wafer fully proccessed facing up

Bonding process

Si wafer and GaAs wafer bonded face to face using "glue" agent

Thinning process

Si wafer with active GaAs layers bonded on top

GaAs OEIC processing

Fully processed optoelectronics interconnected with Si circuits ready for dicing and packaging

Challenges for Crete:

1) GaAs MBE epi-wafers with minimum density of surface defects ("oval" defects)
2) Demonstration of a complete optical interconnection path with the same MQW LD-structure
3) Fabrication of Laser Diode mirrors with Reactive Ion Etching

G. Halkias, D. Tsoukalas, A. Georgakilas, patent GR1003602 (19/06/2001)

Mastering the MQW Laser Diode structures

UoC & FORTH

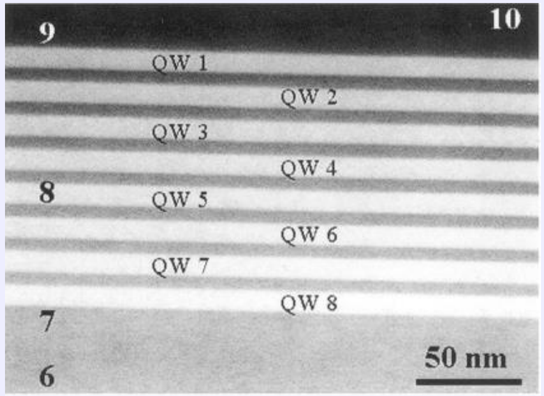

Laser diode structure GRINSCH–MQW:

Graded Index Separate Confinement Heterostructure – Multiple Quantum Well

0.15 μm p^{++} GaAs contact layer

0.1 μm p $Al_xGa_{1-x}As$ graded index layer

0.6 μm p $Al_{0.45}Ga_{0.55}As$ cladding layer

0.24 μm p $Al_{0.26}Ga_{0.74}As$ confinement layer

0.05 μm $Al_xGa_{1-x}As$ graded index layer

MQW structure: 100 A GaAs QW- 60 A $Al_{0.2}Ga_{0.8}As$

0.05 μm $Al_xGa_{1-x}As$ graded index layer

0.24 μm n $Al_{0.26}Ga_{0.74}As$ confinement layer

0.1 μm $Al_xGa_{1-x}As$ graded index layer

1.55 μm n $Al_{0.45}Ga_{0.55}As$ cladding layer

0.1 μm n $Al_xGa_{1-x}As$ graded index layer

n^{++} GaAs substrate

2QW LDs vs. cavity length

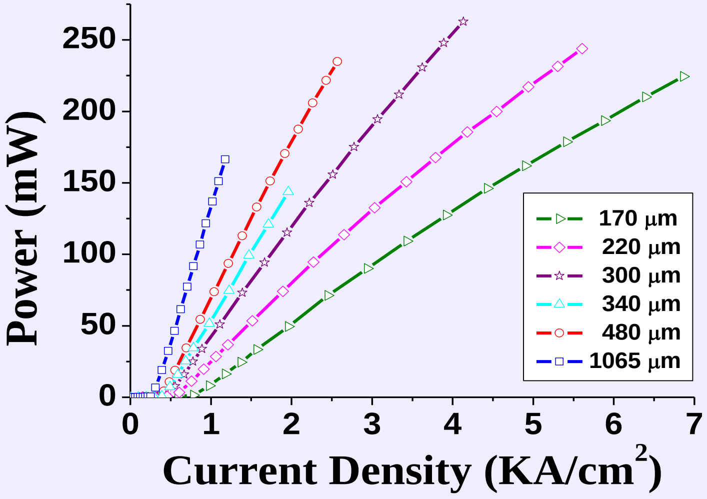

Comparative performance of LDs and PDs vs. number of QWs

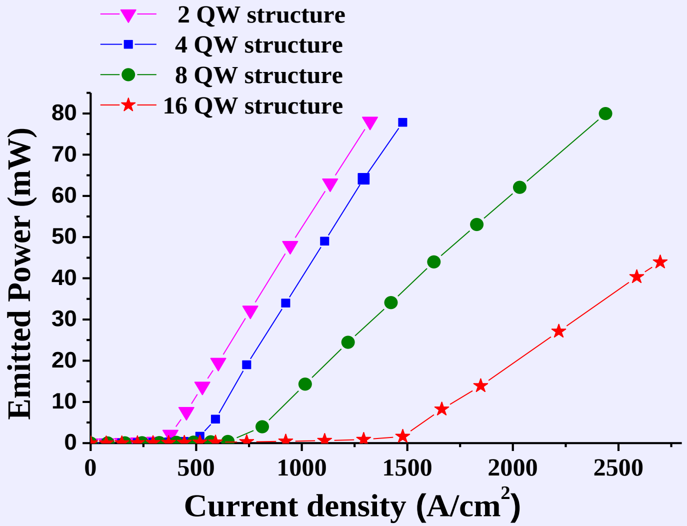

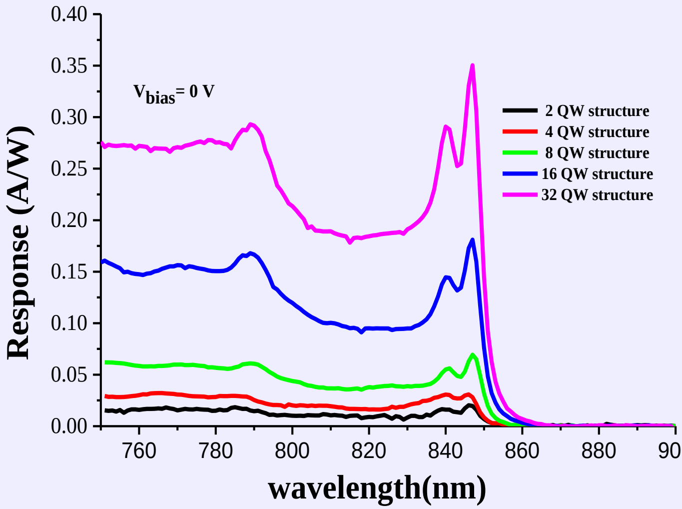

Demonstration of LD-WG-PD GaAs optical link

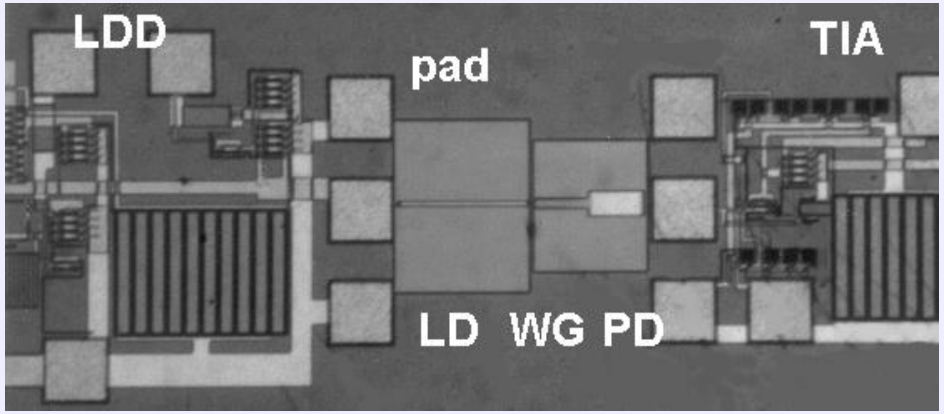

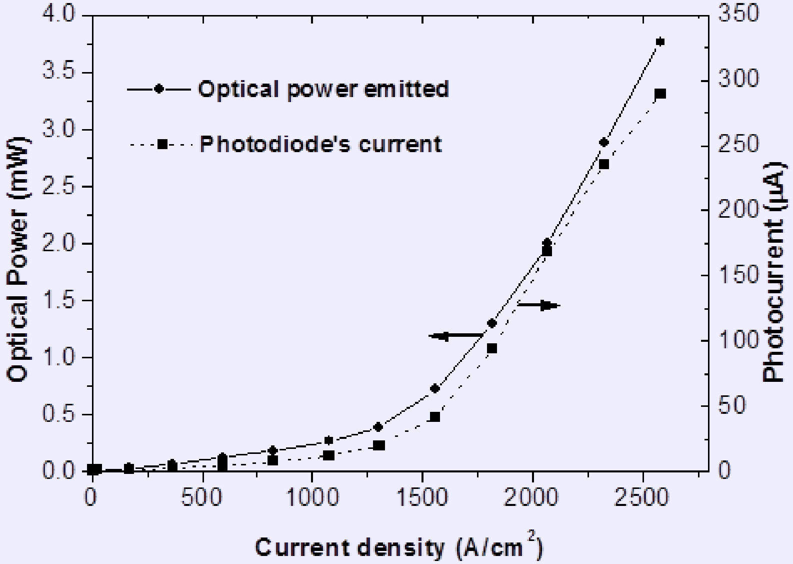

“Wafer-scale integration of GaAs optoelectronic devices with Si ICs using a low temperature bonding procedure”, A. Georgakilas, G. Deligeorgis, E. Aperathitis, D. Cengher, Z. Hatzopoulos, M. Alexe , V. Dragoi, U. Gösele, E. D. Kyriakis-Bitzaros and G. Halkias, Appl. Phys. Lett. 81, 5099 (2002)

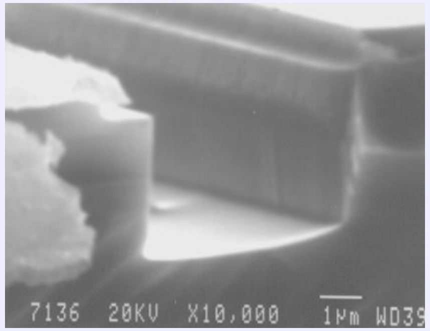

Reactive Ion Etching edge emitting lasers

RIE monitoring by laser interferometry

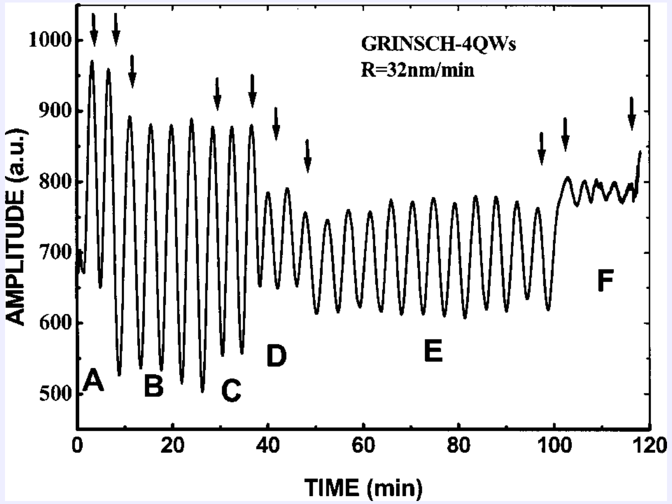

"Laser interferometry as a diagnostic tool for the fabrication of reactive ion etching-edge-emitting lasers”, E. Aperathitis, Z. Hatzopoulos, A. Georgakilas and L. Richeboeuf, J. Vac. Sci. Technol. B20, 1994 (2002)

Heteroepitaxy of GaAs-on-Si

- ✓ **The high-lattice mismatch and polar-on-nonpolar heteroepitaxial system of GaAs-on-Si has been extensively investigated (PhD thesis, 1990)**
- ✓ **Significant understanding in the physics of heteroepitaxy, the material properties and the potential for devices' development has been acquired - state-of-the-art material was achieved**
- ✓ **GaAs-on-Si know-how was transferred to a Si wafer manufacturer (ESPRIT 9500, German Special Action)**
- ➢ **In GaAs-on-Si, late Prof. John Stoemenos was my key collaborator and teacher, alongside Profs. Aris Christou and Zack Hatzopoulos. He inspired my interest on the structural properties and their interrelation with the electronic properties of III-V semiconductor interfaces and thin films**

"Achievements and Limitations in Optimized GaAs Films Grown on Si by Molecular Beam Epitaxy", A. Georgakilas, P. Panayotatos, J. Stoemenos, J.-L. Mourrain, and A. Christou, J. Appl. Phys. 71, pp. 2679-2701 (1992)

"Generation and annihilation of antiphase domain boundaries in GaAs on Si grown by molecular beam epitaxy", A. Georgakilas, J. Stoemenos, K. Tsagaraki, Ph. Komninou, N. Flevaris, P. Panayotatos, and A. Christou, J. Mater. Res. 8, pp. 1908-1921 (1993)

"Alloy clustering and defect structure in the molecular beam epitaxy of $In_{0.53}Ga_{0.47}As$ on Silicon", A. Georgakilas, A. Dimoulas, A. Christou, and J. Stoemenos, J. Mater. Research 7, pp. 2194-2204 (1992)

Polar on nopolar epitaxy / APBs in GaAs-on-Si

UoC & FORTH

Single-atom height steps on the Si surface result to Antiphase Domain Boundaries (APBs)

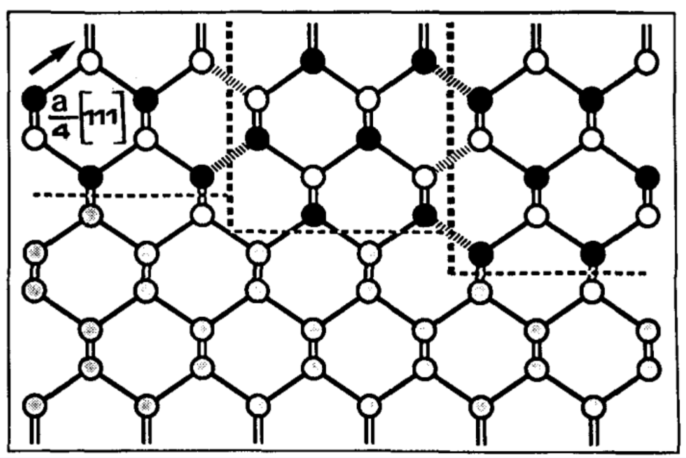

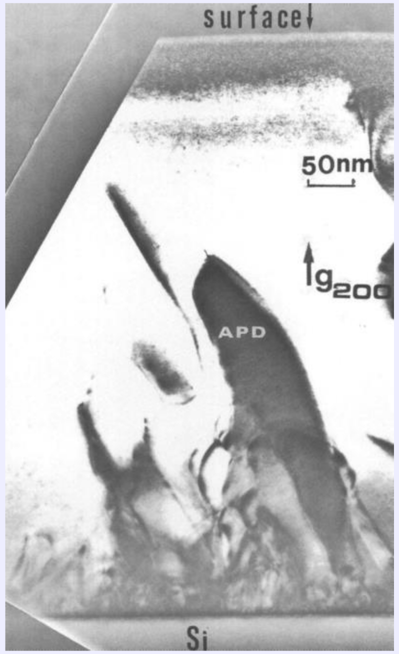

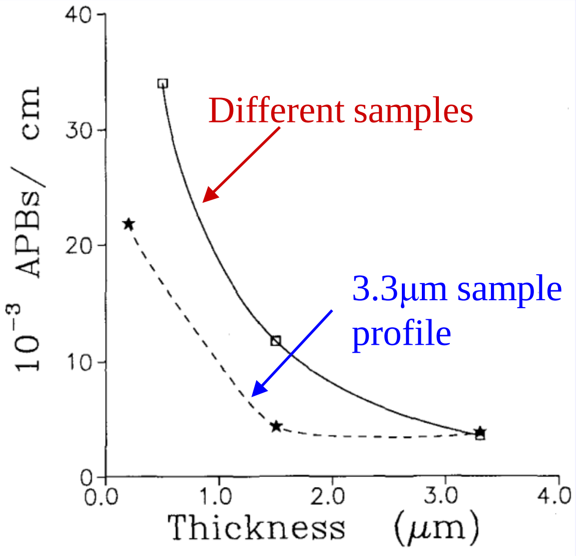

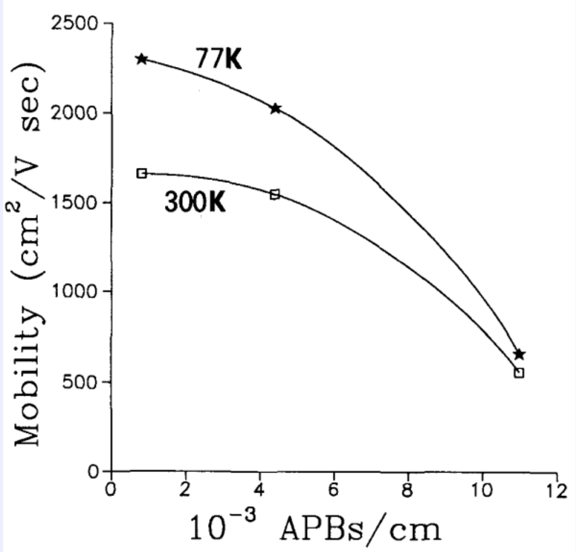

Chemical stain for APDs/APBs

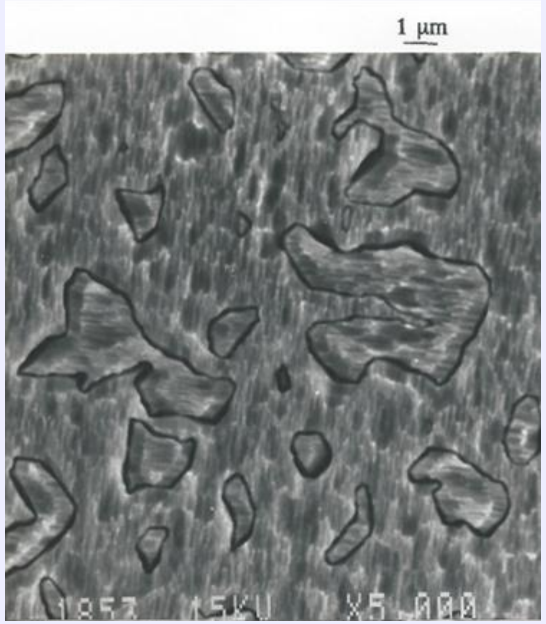

Our systematic study has well documented that APBs always exist at the interface but are annihilated with increasing epilayer thickness

This however depends on the selection of Si (001) off misorientation - and details (T_{sub}) of exposure of clean Si to As or contamination

APBs degrade the electron mobility and increase leakage currents

A. Georgakilas et al, J. Mater. Res. 8, 1908 (1993)

State-of-art GaAs-on-Si

A. Georgakilas et al, J. Appl. Phys. 71, 2679 (1992)

- ✓ **Epitaxial Si prior to GaAs-on-Si epitaxy optimized its microstructure and surface smoothness**
- ▪ **1 μm GaAs/Si with record low XRD (004) FWHM=255 arcsec**
- ▪ **Threading dislocation density ~10^8 cm^{-2}**

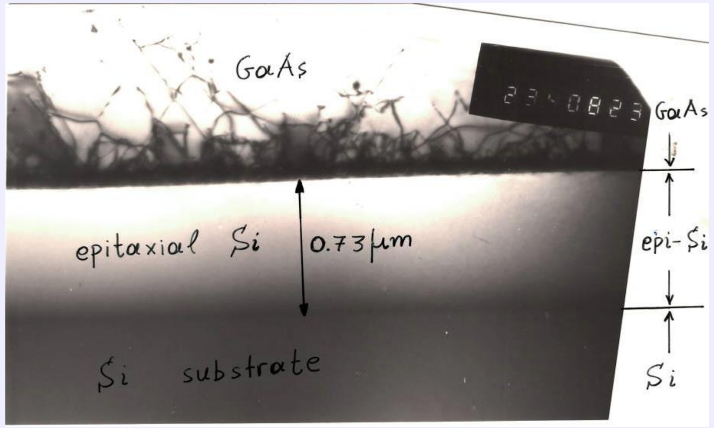

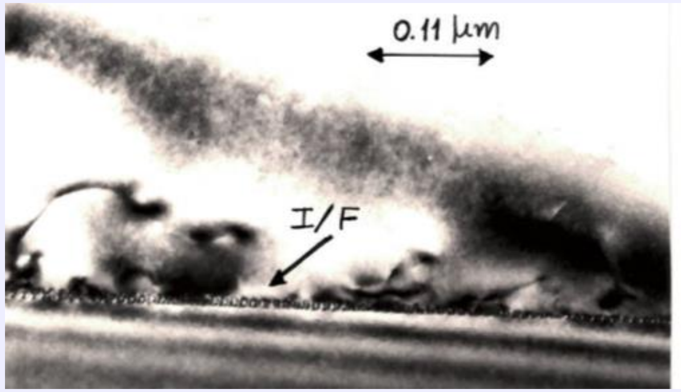

A. Georgakilas et al, IEEE Trans. Elect. Dev. 40, 507 (1993)

- ✓ **MESFET Lg=1.3μm, Wg=180μm**
- ▪ **Maximum g_m= 227 mS/mm**
- ▪ **f_T=18 GHz, f_{max}=30 GHz**

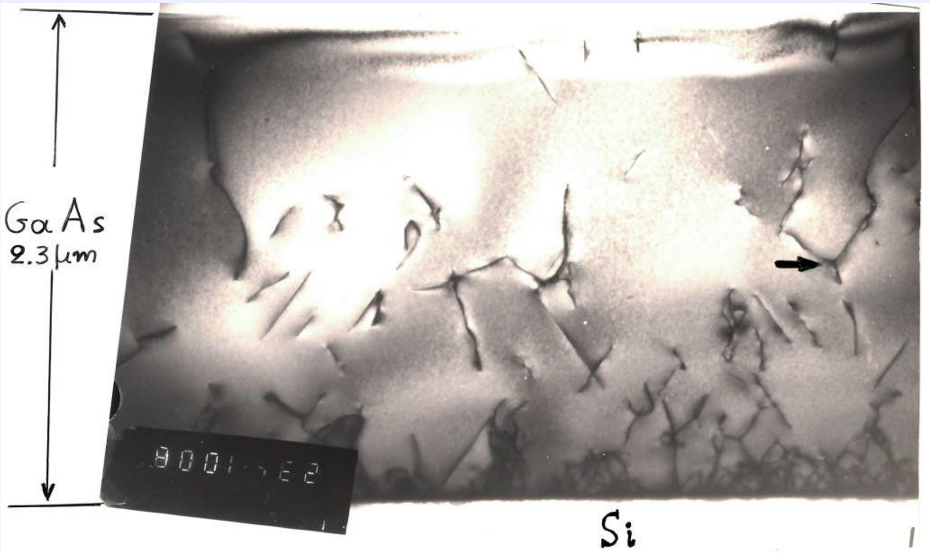

"Investigation of the GaAs/Si Heterojunction Band Lineup with Capacitance and Current Versus Voltage Measurements", A. Georgakilas et al, Mater. Sci. Eng. B44, 383 (1997)

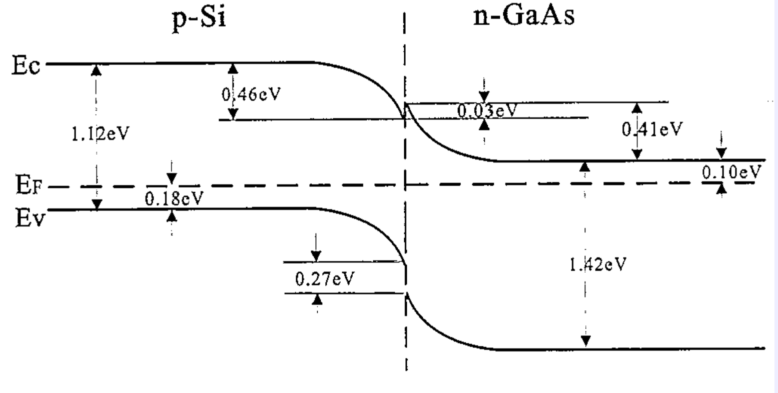

Fig. 3. Energy band diagram for the n-GaAs/p-Si heterojunction with $n \approx p \approx 10^{16}$ cm^{-3}, stemming from $C-V$ intercept results.

III-Nitride Semiconductors

Map of III-Nitrides PAMBE research

Heteroepitaxy on different substrates

GaAs (001)

Al_2O_3
(0001) c-plane
$(1\bar{1}02)$ r-plane

Si (111) etc.

Diamond
(111), (100), (110)
& polycrystalline

GaN-based HEMTs

AlGaN barrier
ISFET/CHEMHEMTs
Double-heterojunction

AlN barrier
Double-heterojunction
and thin buffer

In-containing III-Nitrides

InN

Quaternary
$In_xAl_yGa_{1-x-y}N$
GaN/InAlGaN QWs

Ternary
$In_xGa_{1-x}N$

Ternary
$In_xAl_{1-x}N$

III-Nitride Nanowires

Self-organized
GaN NWs

Patterned
GaN NWs

Self-organized
InN NWs

Spontaneous
InGaN NWs

Control of GaN polarity on Al_2O_3 (0001)

UoC & FORTH

The effect of Sapphire's nitridation on the polarity of overgrown GaN layers was determined

100 min Nitridation

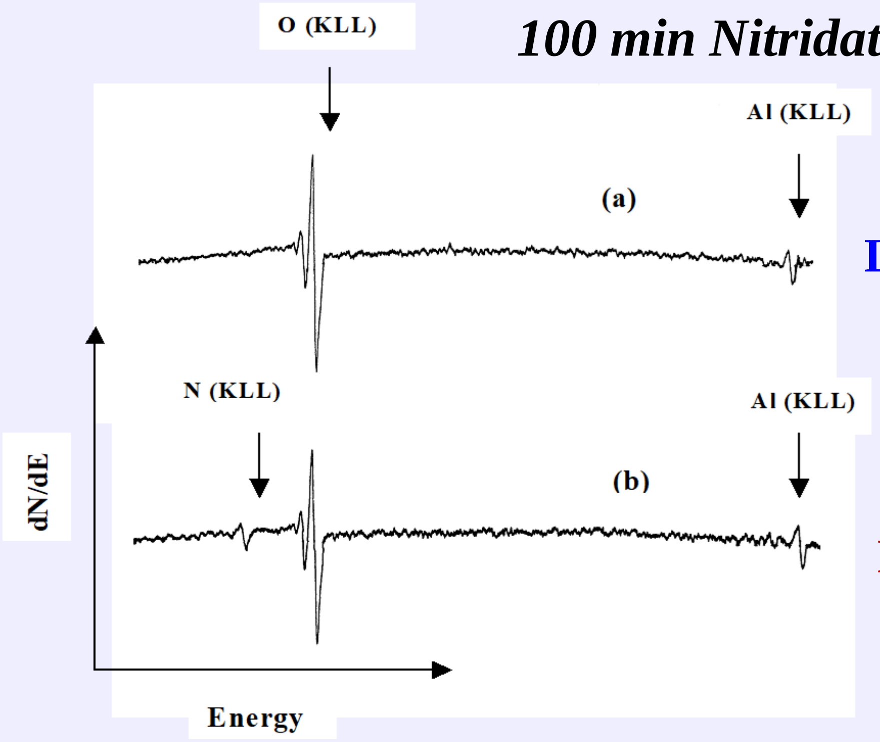

Low T_{sub} ~200°C

High T_{sub} ~750°C

No interfacial AlN layer for low T_{sub} →
N-face epilayer with cubic regions near the IF

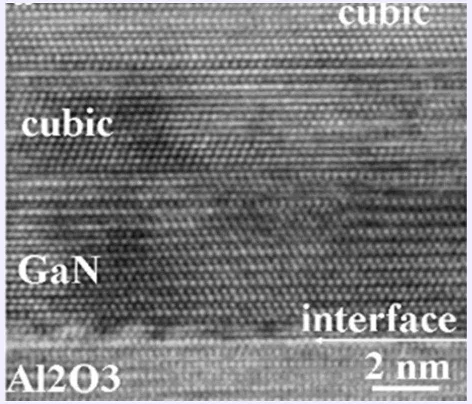

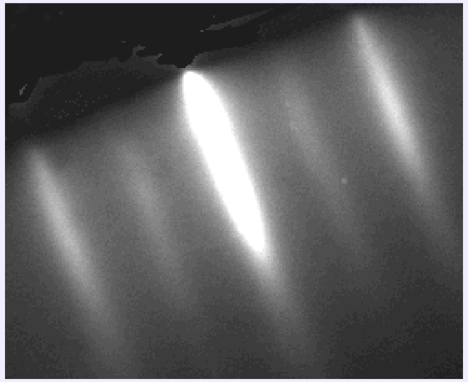

x2

RHEED patterns in [11$\bar{2}$0] azimuth

~1.5 nm (6 ML) IF AlN layer for high T_{sub} →Ga-face epilayer

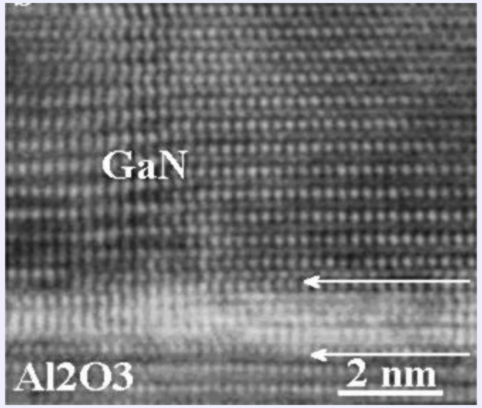

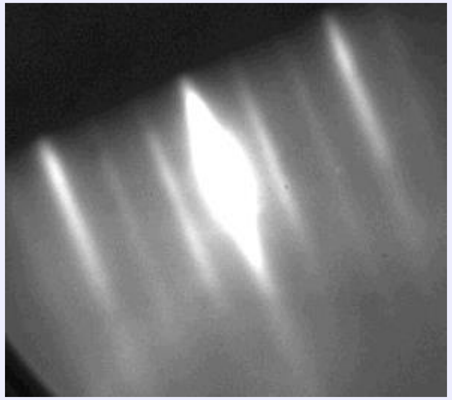

x3

For Ga-polarity epilayers, we adopted Low T nitridation and AlN nucleation layer

S. Mikroulis et al, Appl. Phys. Lett. 18, 266 (2002)
A. Georgakilas et al, Phys. Stat. Solidi (a) 188, pp. 567-570 (2001)

Control of GaN polarity and orientation on Diamond

- **Studying the growth of GaN-on-diamond we found that the III-Nitride polarity depends on the thickness of AlN nucleation layer. This is also applicable in GaN-on-Si**
- **Ga-face (0001) orientation is possible for all orientations of polycrystalline diamond substrates**

"Method for heteroepitaxial growth of III metal-face polarity III-Nitrides on substrates with diamond crystal structure and III-nitride semiconductors», **A. Georgakilas, K. Aretouli and K. Tsagaraki, GR1008013 (22.10.2013), US 10,192,737 B2 (29.01.2019) and EP 2 842 154 B1 (25.03.2020)**

2 nm AlN on diamond

↓

(0001)
Metal-face

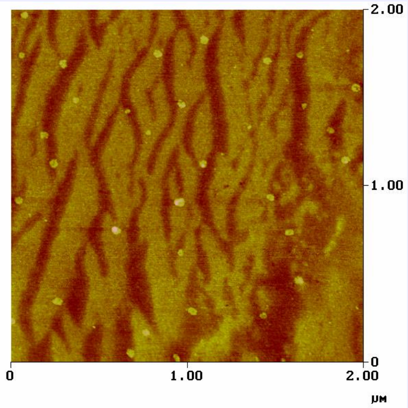

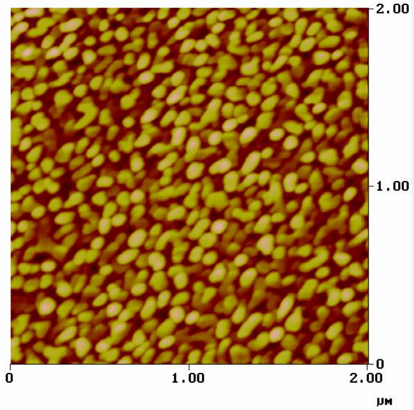

70 nm AlN on diamond

↓

$(000\bar{1})$
N-face

Similar morphology across GBs, no change with KOH

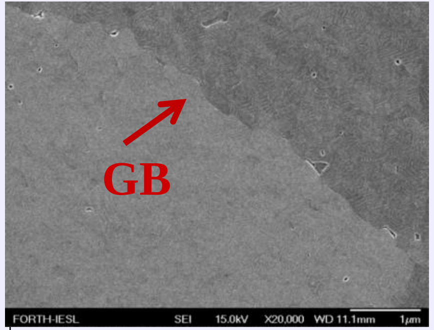

- **Change of polarity should result from (0001) IDBs at 3D-islands**

(0001) Al-Al IDB or C(Si) impurities ?

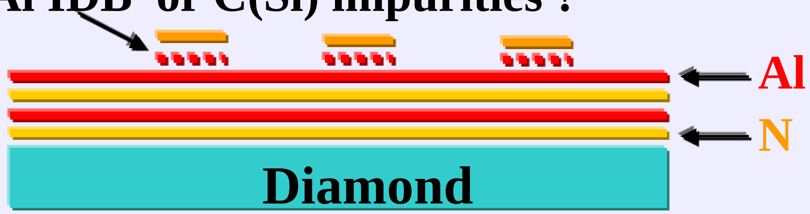

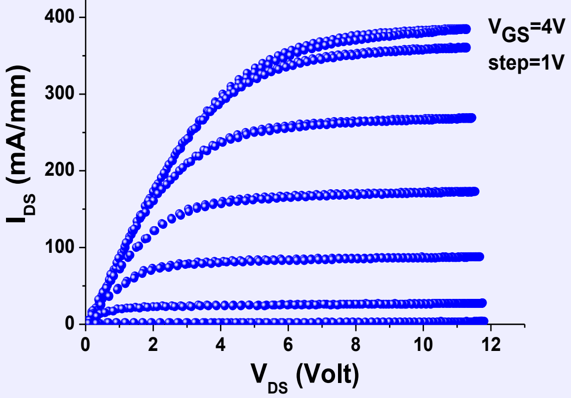

Control of GaN polarity and orientation on Si

UoC & FORTH

- **The AlN nucleation layer thickness effect on (0001) orientation and polarity has been confirmed also for GaN-on-Si (111), (100), (110) & (211) substrates**
  - **XRD confirmed the {0001} III-Nitride orientation**
  - **KOH etching confirmed the Ga-face polarity**

AlN/GaN HEMT on Si (111)

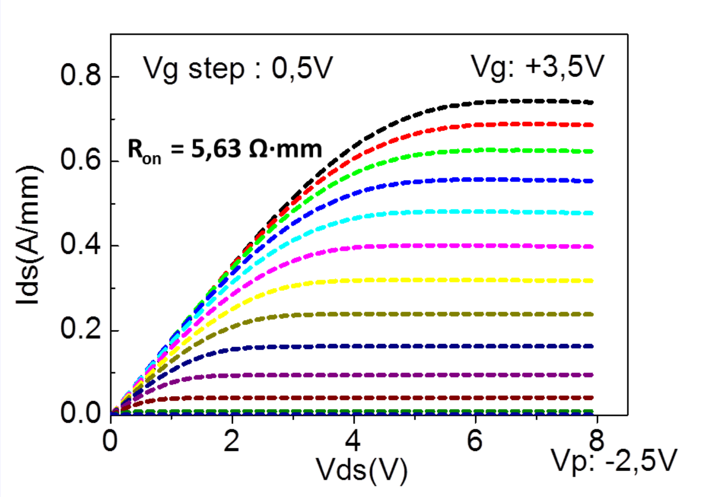

A. Adikimenakis et al, Poster P1.57

GaN/1.7 nm AlN on Si (110) 4° off

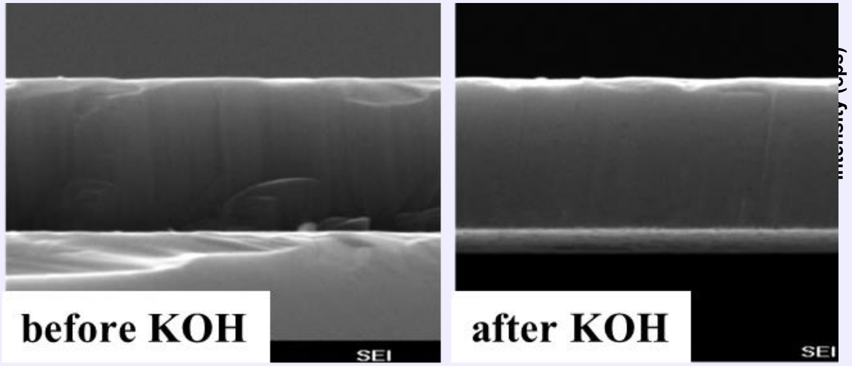

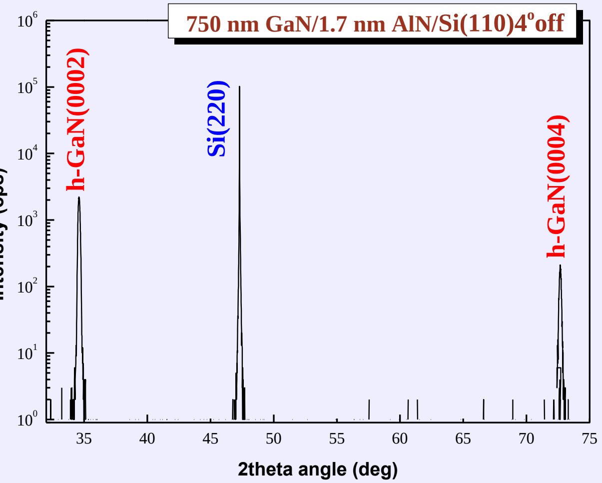

GaN/1.7 nm AlN on Si (100) 1.5° off

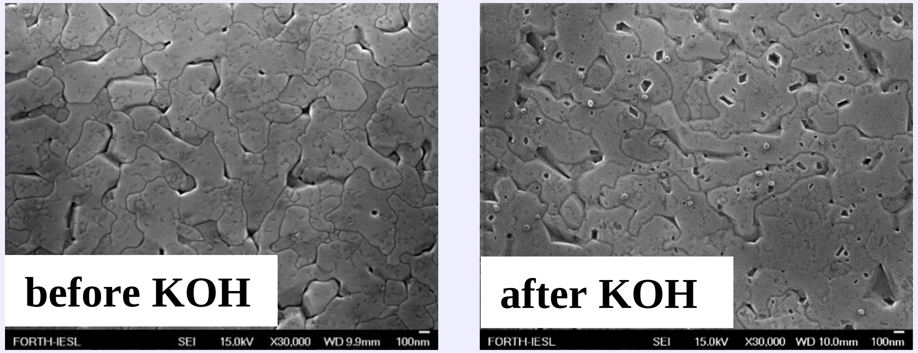

Our favorite AlN/GaN HEMT system

UoC & FORTH

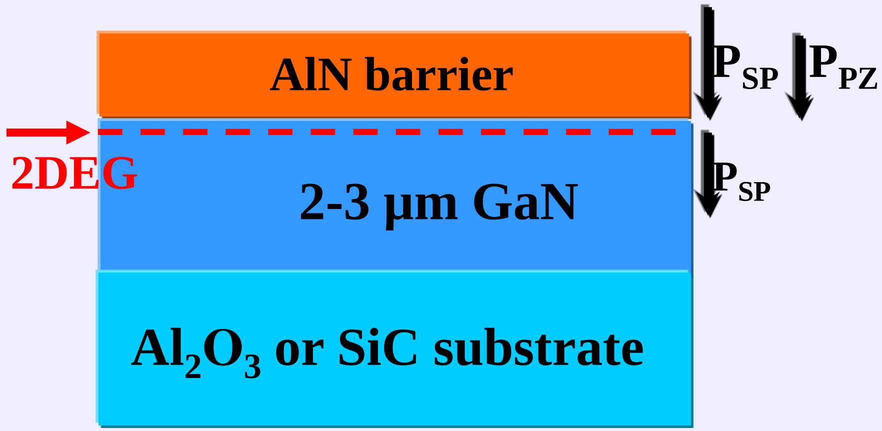

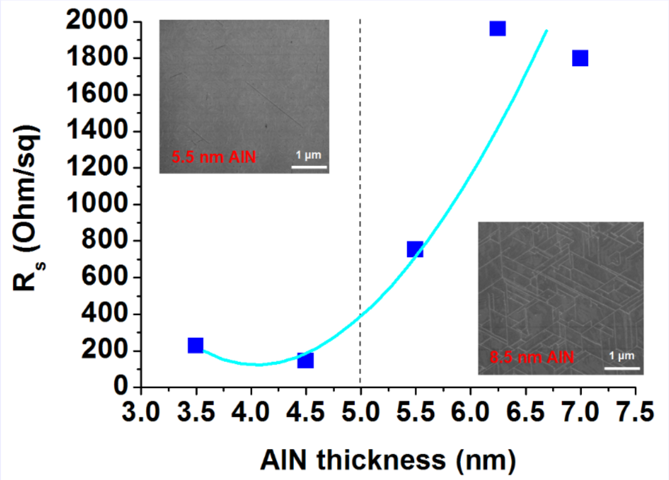

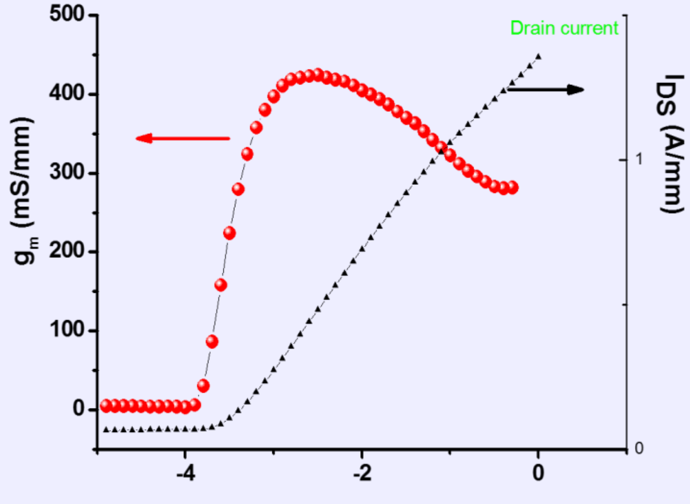

A. Adikimenakis et al at MNE 2008; Microel. Eng. 86, 1071 (2009)

Record low sheet resistance

- At 300K, R_s= 144 Ohm/sq, N_s= 3.6×10^{13} cm^{-2}, μ = 1200 cm^2/Vs
- At 77K, R_s= 52 Ohm/sq, N_s= 3.0×10^{13} cm^{-2}, μ = 4000 cm^2/Vs

Double Heterojunction, thin AlN buffer

A. Bairamis et al, Appl. Phys. Lett. 105, 113508 (2014

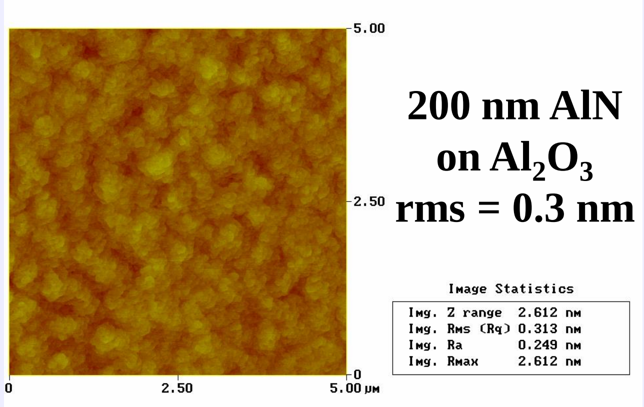

200 nm AlN
on Al_2O_3
rms = 0.3 nm

Image Statistics

Img. Z range	2.612 nm
Img. Rms (Rq)	0.313 nm
Img. Ra	0.249 nm
Img. Rmax	2.612 nm

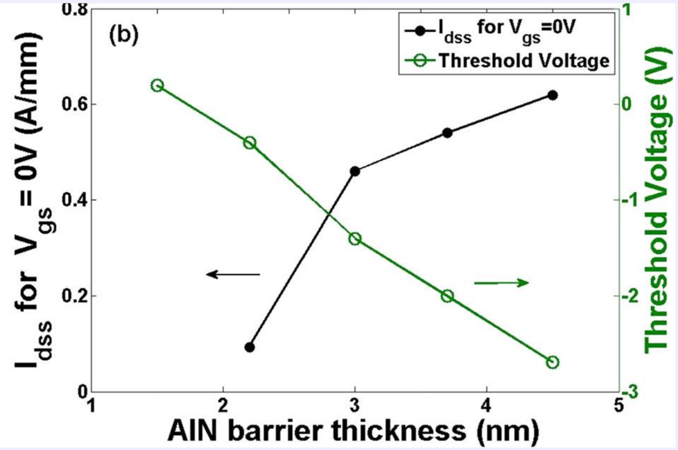

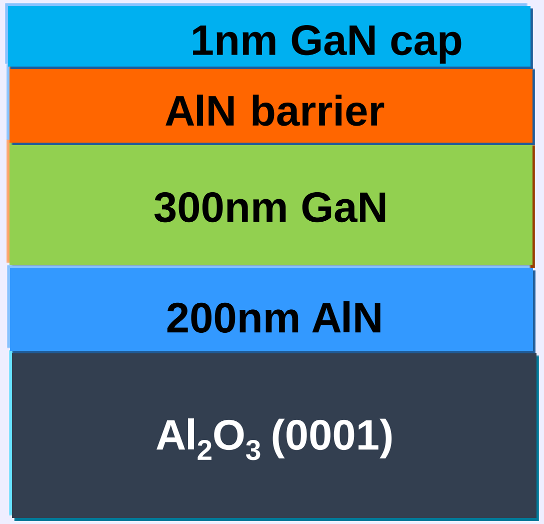

Growth of In-containing III-Nitrides

- Growth of In-containing III-nitrides requires precise and reproducible control of T_{sub}
- A method based on RHEED was invented
  - Few ML In or InN is deposited at low T_{sub}, then T_{sub} is increasing under N and In atoms desorb
  - A **1x3 RHEED pattern** corresponding to **(√3x√3)R30°** surface reconstruction is observed (T_{sub} ~ 520°C)

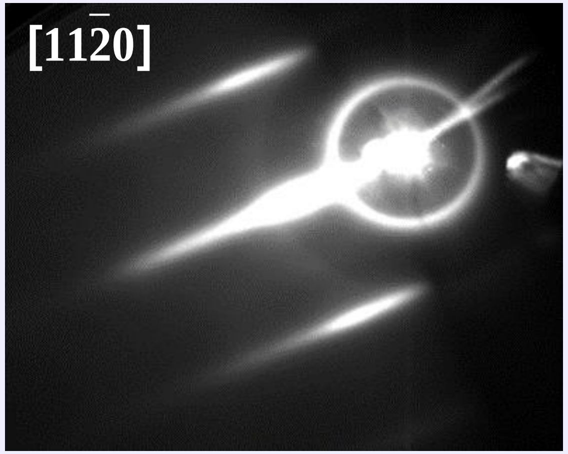

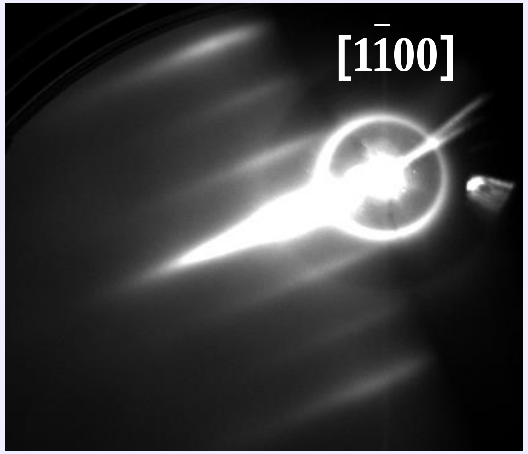

“Growth of nitride semiconductor heterostructures including Indium Aluminum Gallium Nitride alloy layers by the method of Molecular Beam Epitaxy with Nitrogen Plasma Source”, A. Georgakilas, E. Dimakis and N. Pelekanos, GR1004675 (13.09.2004)

Experiments for InN growth

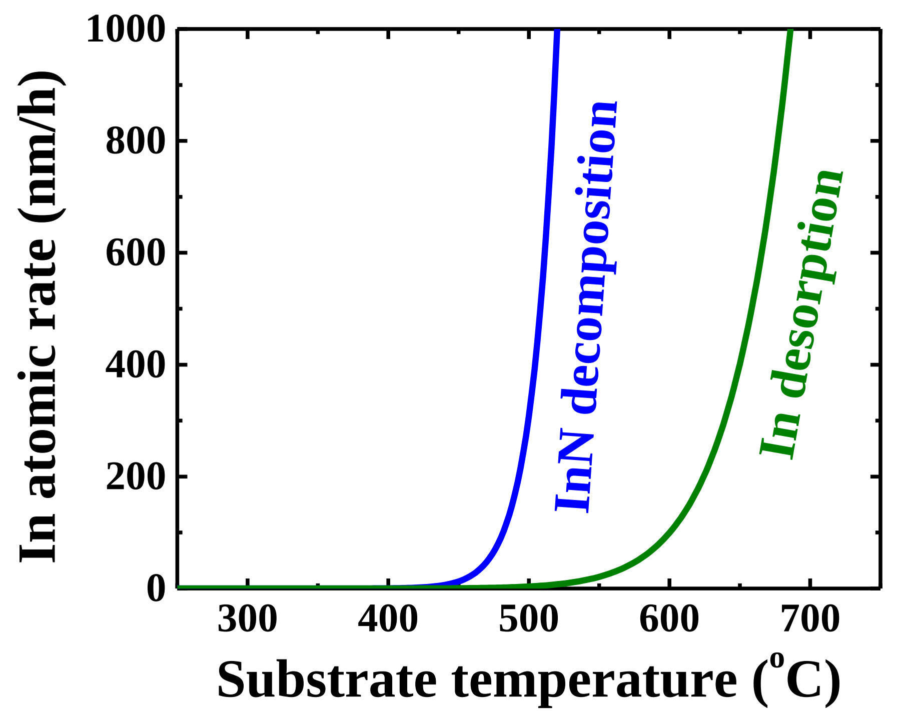

E. Dimakis et al., J. Appl. Phys. 97, 113520 (2005)
E Dimakis et al., Superl & Microstr 36, 497 (2004)

Quaternary InAlGaN and InAlGaN/GaN QWs

The concept – Nikos Pelekanos

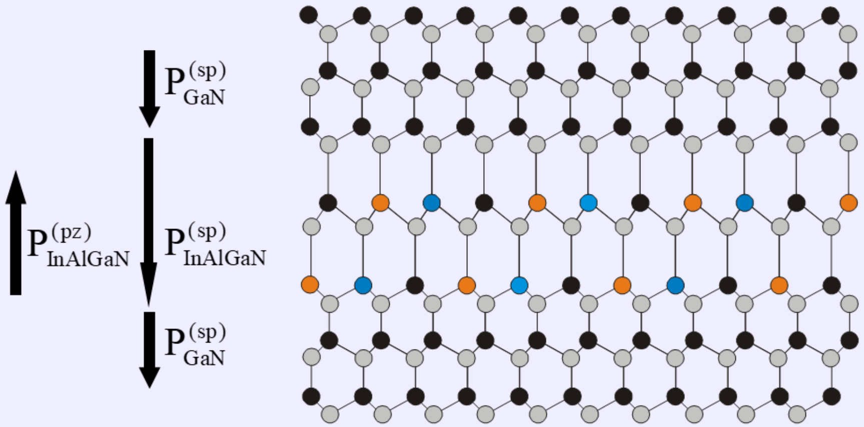

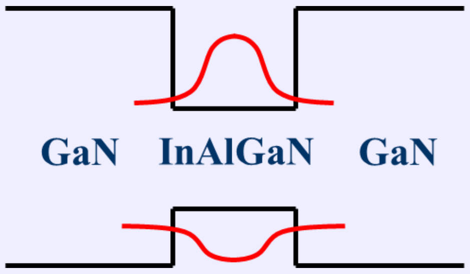

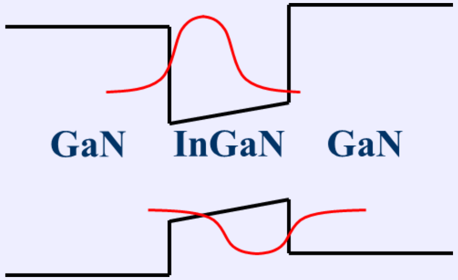

Extensive growth experiments

$$F_{Ga}+F_{Al}=0.35\ \mu m/h < F_N= 0.40\ \mu m/h < F_{Ga}+F_{Al}+F_{In}= 0.45\ \mu m/h$$

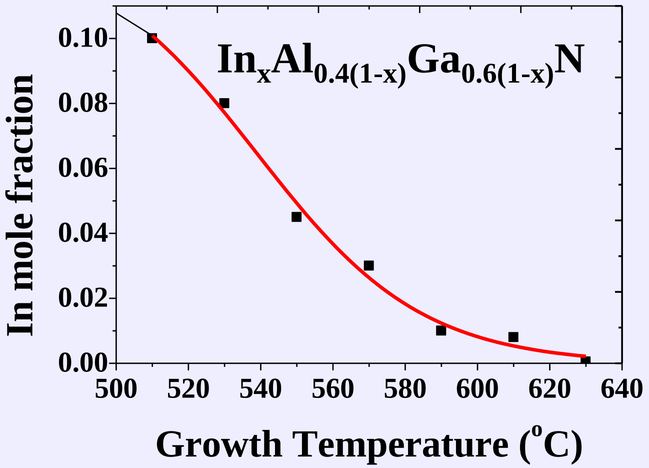

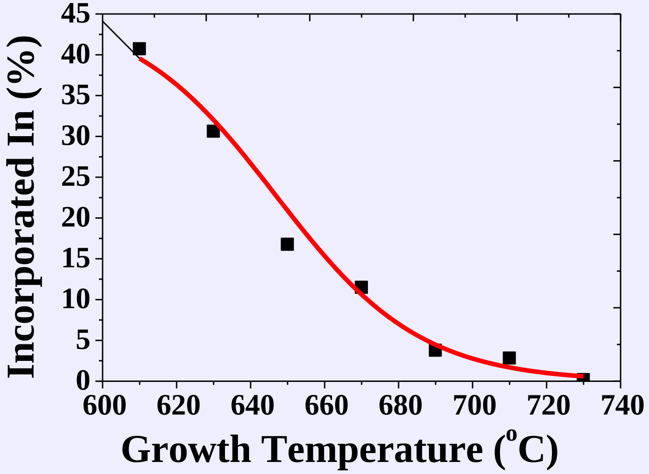

0.1 µm $In_{0.13}Al_{0.30}Ga_{0.57}N$

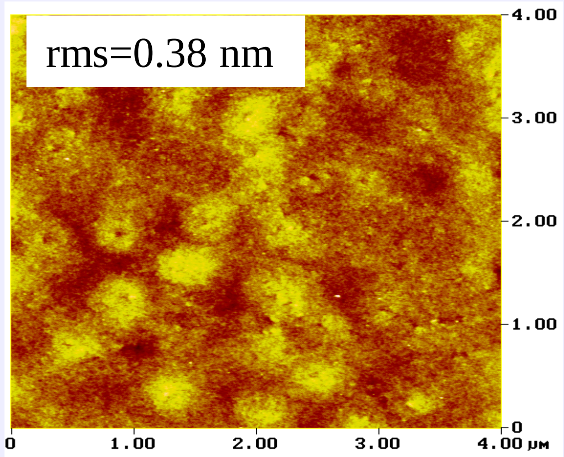

x10 {8nm $In_{0.08}Al_{0.31}Ga_{0.61}N$/ 3nm GaN}

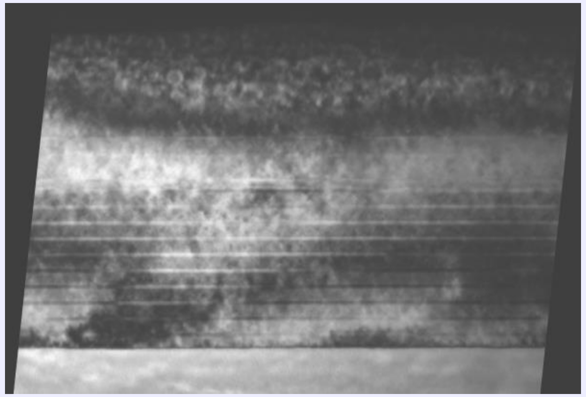

InAlGaN Bandgap and InAlGaN/GaN QW emission

UoC & FORTH

In-bowing parameter of $In_xAl_yGa_{1-x-y}N$ alloys for various In and Al compositions

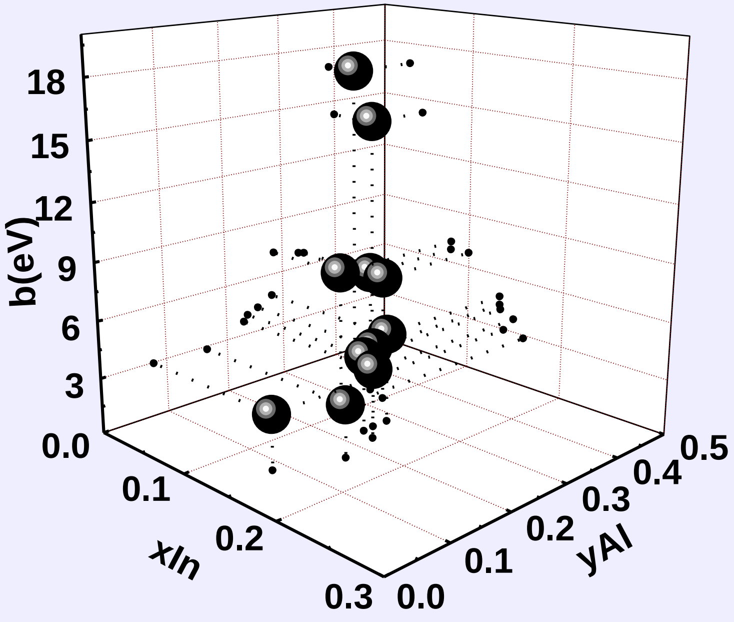

M. Androulidaki et al,
Phys. Stat. Solidi (c) 0, 507 (2002)

58 meV PL linewidth at 300K for GaN/InAlGaN/GaN QW

Lasing under optical pumping at 300K

Lasing lines above a threshold between $0.32P_0$ and $0.5P_0$, $P_0 \sim 1MW/cm^2$

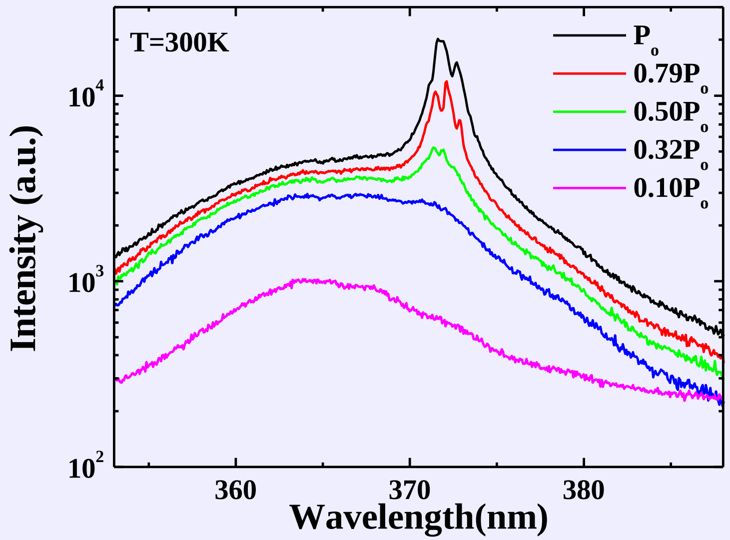

E. Dimakis et al,
J. Cryst. Growth 251, 476 (2003)

Zero field $In_{0.14}Al_{0.28}Ga_{0.58}N$ /GaN QWs

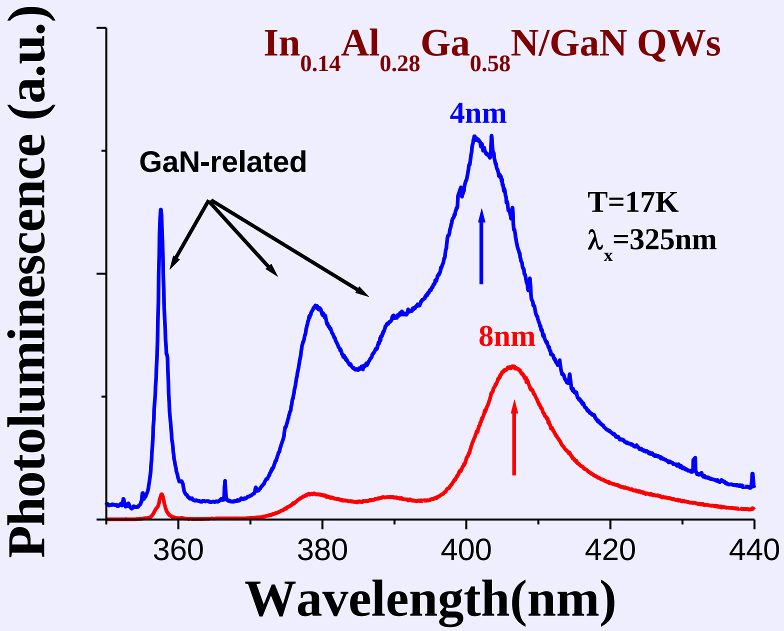

F. Kalaitzakis et al,
Phys. Stat. Sol. (b) 240, 301 (2003)

InAlN and InGaN alloys – Bandgap dependencies

UoC & FORTH

Far from equilibrium PAMBE enables the growth of $In_xGa_{1-x}N$ and $In_yAl_{1-y}N$ alloys in the entire composition range

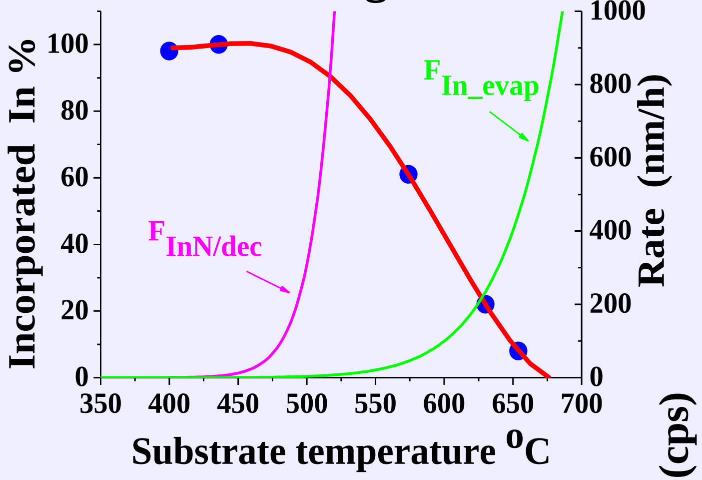
InAlN growth

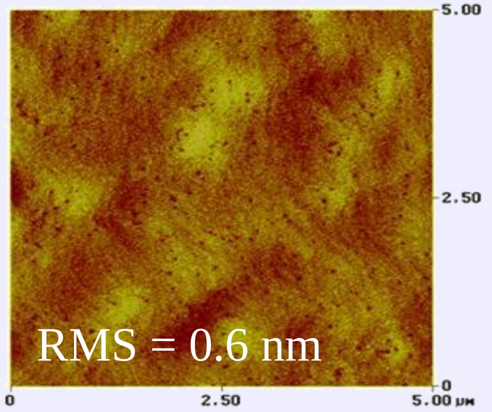

RMS = 0.6 nm

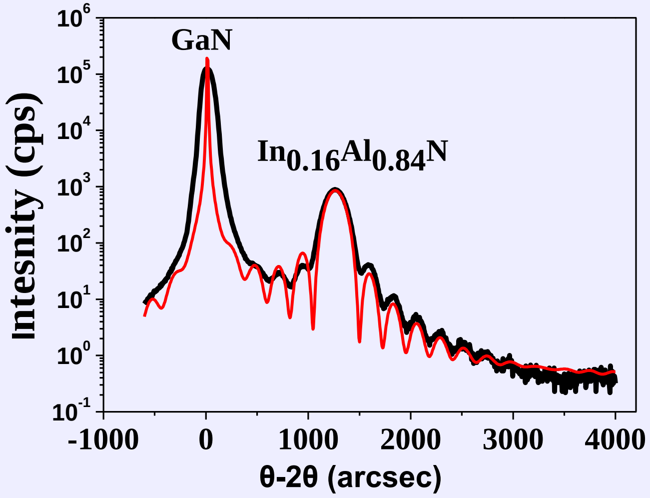

PAMBE grown InAlN and InGaN alloys have been used to determine the bandgap dependence on composition

$$E_{gap}(In_xAl_{1-x}N) = x\cdot E_{gap}(InN) + (1-x)\cdot E_{gap}(AlN) - b\cdot x\cdot(1-x)$$

$$b(x) = \frac{a}{1+\beta\cdot x}$$

$$a = 15.3 \pm 1.6\ eV$$

$$\beta = 4.8 \pm 0.9$$

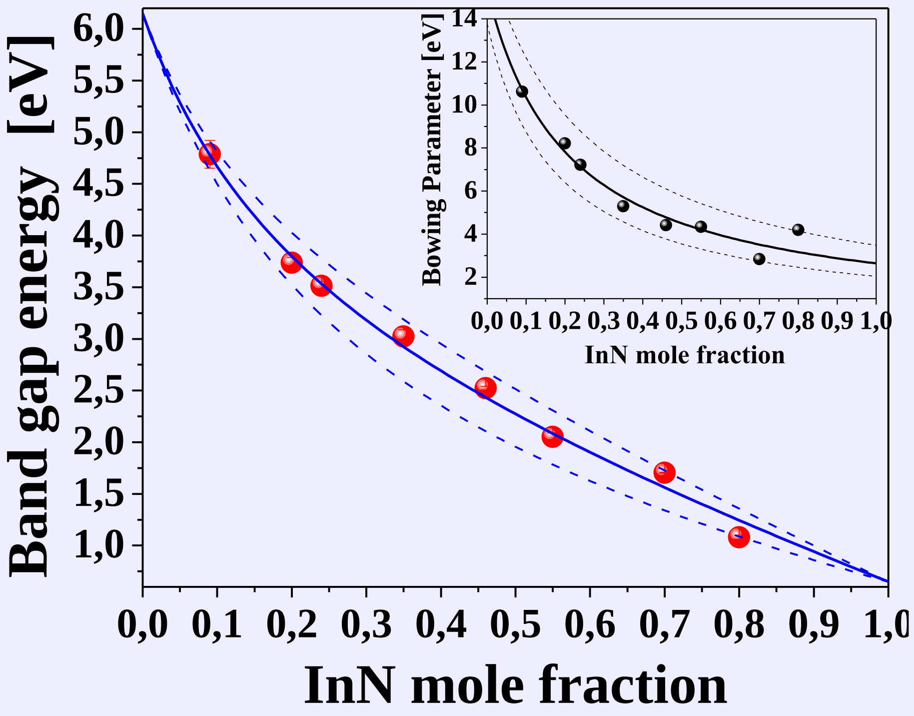

InAlN → E. Iliopoulos et al, Appl. Phys. Lett. 92, 191907 (2008)
InGaN → E. Iliopoulos et al, Phys. Stat. Sol. (a) 203, 102 (2006)

Physical model of InN (0001) growth

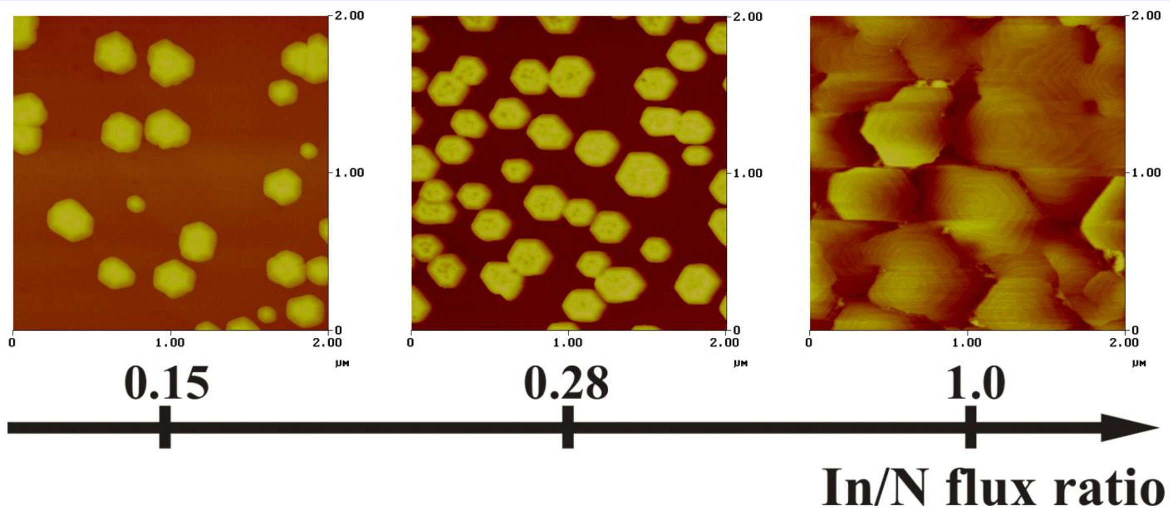

- The coverage of GaN substrate by InN is controlled by the In/N flux ratio
  - 3D islands for $F_{In}/F_N < 1$
  - 2D growth for $F_{In}/F_N \approx 1$

E. Dimakis et al., Appl. Phys. Lett 86, 133104 (2005)

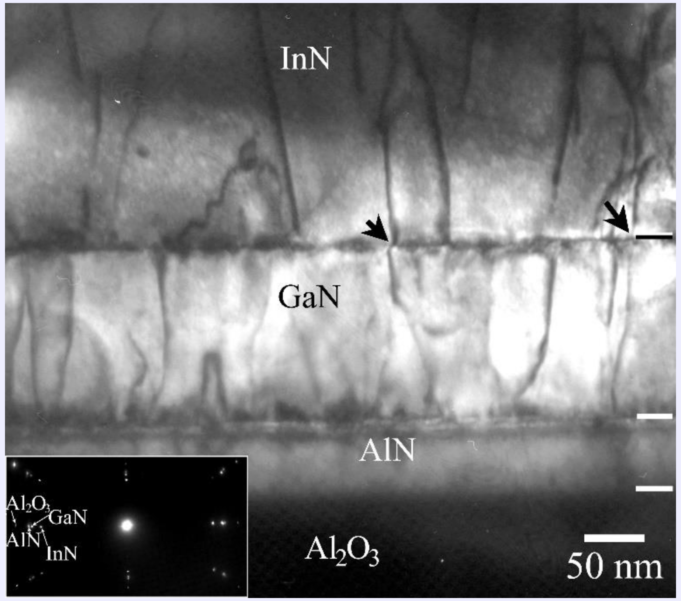

10μm InN film has been grown with atomically smooth surface (using $F_{In}/F_N \approx 1$)

	Pure Edge (cm^{-2})	Pure Screw (cm^{-2})	Mixed (cm^{-2})
Interface	1.55×10^{10}	4.82×10^{8}	1.69×10^{9}
Middle	9.46×10^{9}	4.74×10^{8}	9.48×10^{8}
Surface	4.35×10^{9}	4.80×10^{8}	1.20×10^{9}

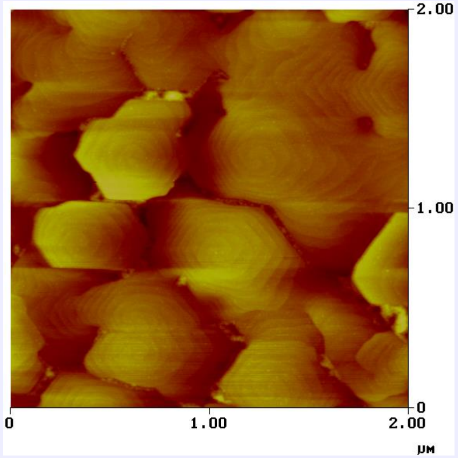

E. Dimakis et al, Superl. Microstr. 40, 246 (2006)

InN biaxial strain and lattice constants

- ✓ **Biaxial relaxation coefficient $(2C_{13}/C_{33}) = 0.43\pm0.04$**
- ✓ **Strain-free lattice parameters:**
  $\alpha = 3.535\pm0.005$Å, $c = 5.699\pm0.004$Å

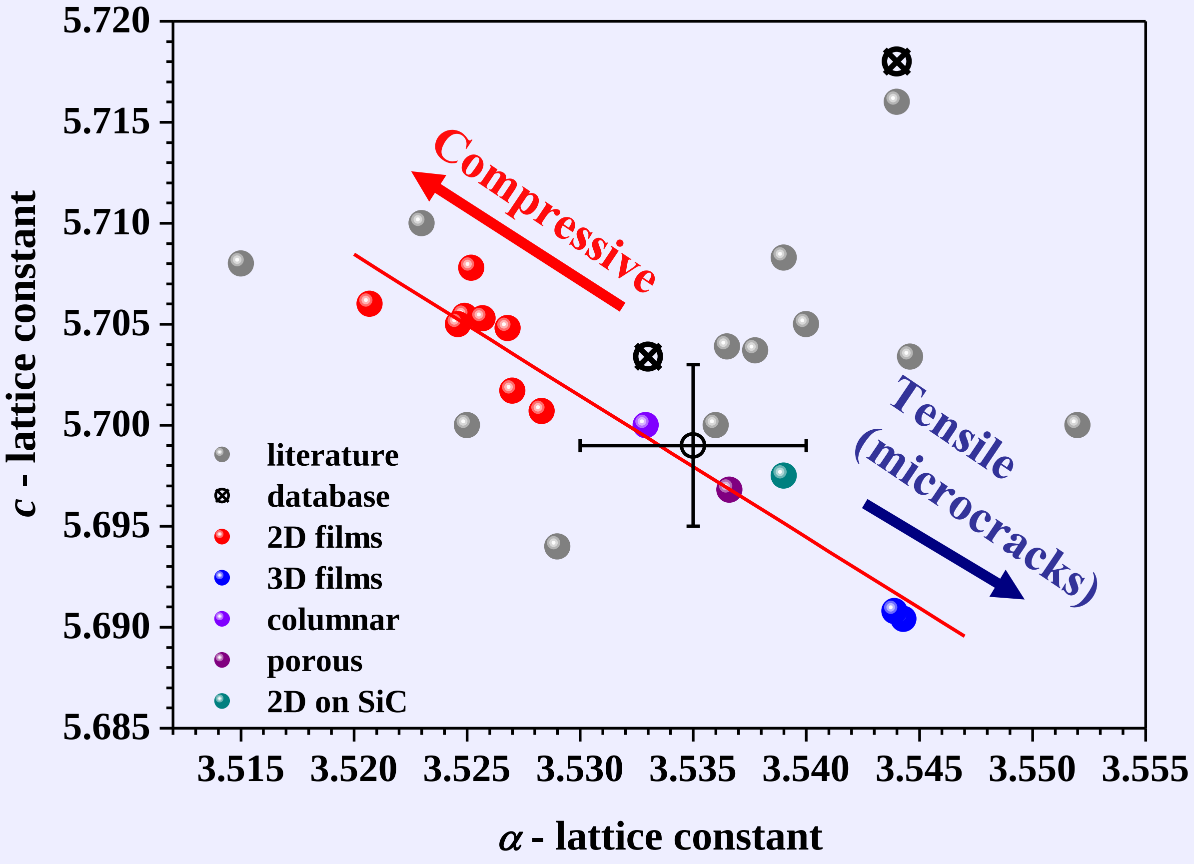

E. Dimakis et al., Appl. Phys. Let. 88, 191918 (2006)

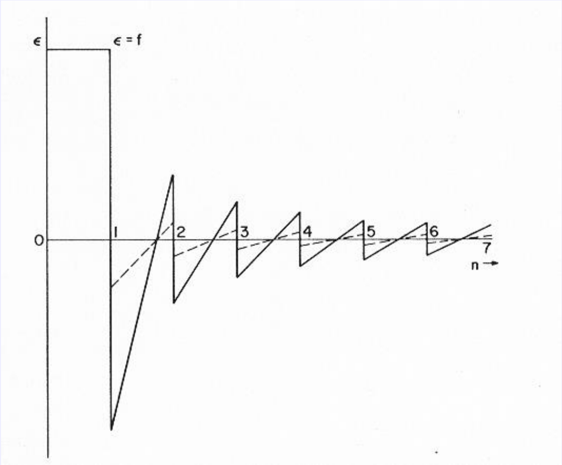

Gradual creation of MD at the edges of misoriented islands during their growth, J. W. Mathews, Epitaxial growth B, ch.8 (1975)

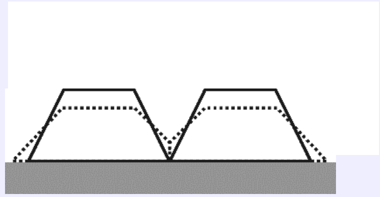

Elastic deformation of misaligned adjacent islands in order to close the gap between them [for GaN/Al_2O_3, T.Bottcher et al APL 78(2001)1976]

InN growth optimization

- ✓ **The effects of T_{sub} within the upper 30°C possible range and InN growth rate were evaluated by structural (plan-view and cross-sectional TEM, HRXRD) and electrical (Hall-effect) analysis**
- ✓ **The bulk InN electron concentration and mobility values were extracted for ~700 nm films**
- ➢ **Results consistent with introduction of defects at coalescence of 2D-like islands**
- ➢ **InN films ~700 nm exhibit electron mobility >2,000 cm^2/Vs and concentration ~5 × 10^{17} cm^{-3}, although treading dislocation density (TDD) is >10^{10} cm^{-2}**

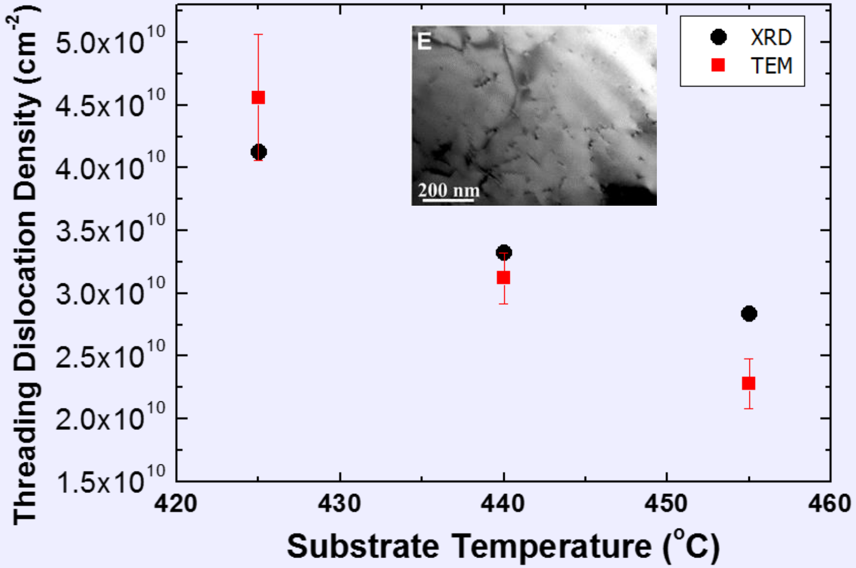

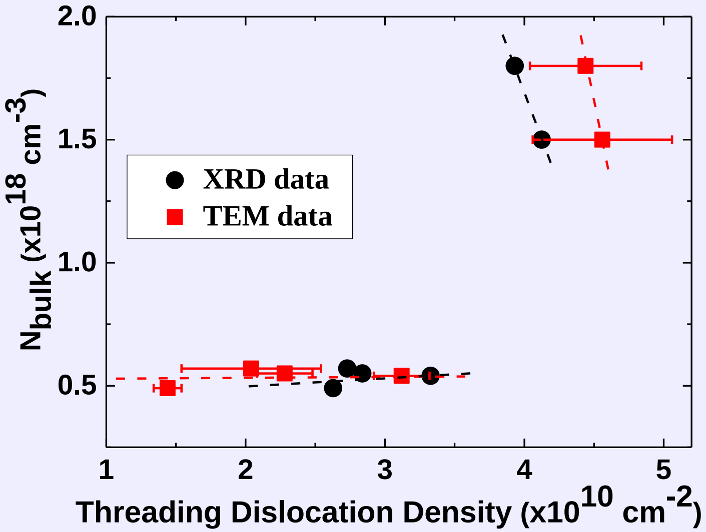

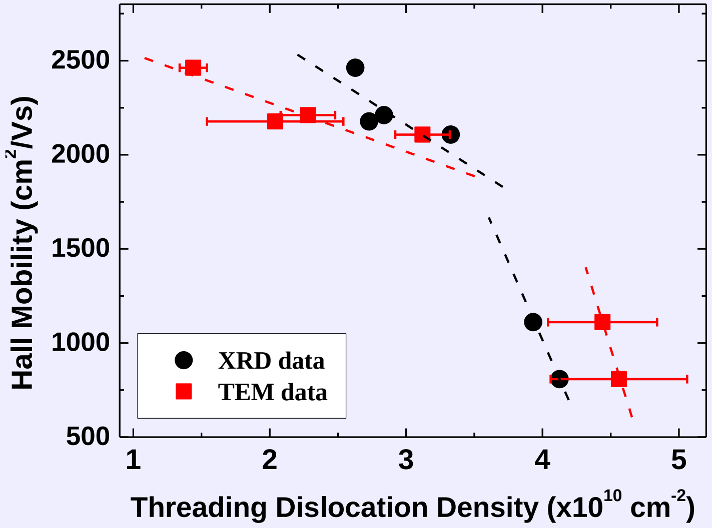

A. Adikimenakis et al., ECS J. Sol. St. Techn. 9, 015006 (2020)

About InN Unintentional Donors and Bandgap

- ✓ *Threading Dislocations are unlikely to be the exclusive source of unintentional Donors in InN*

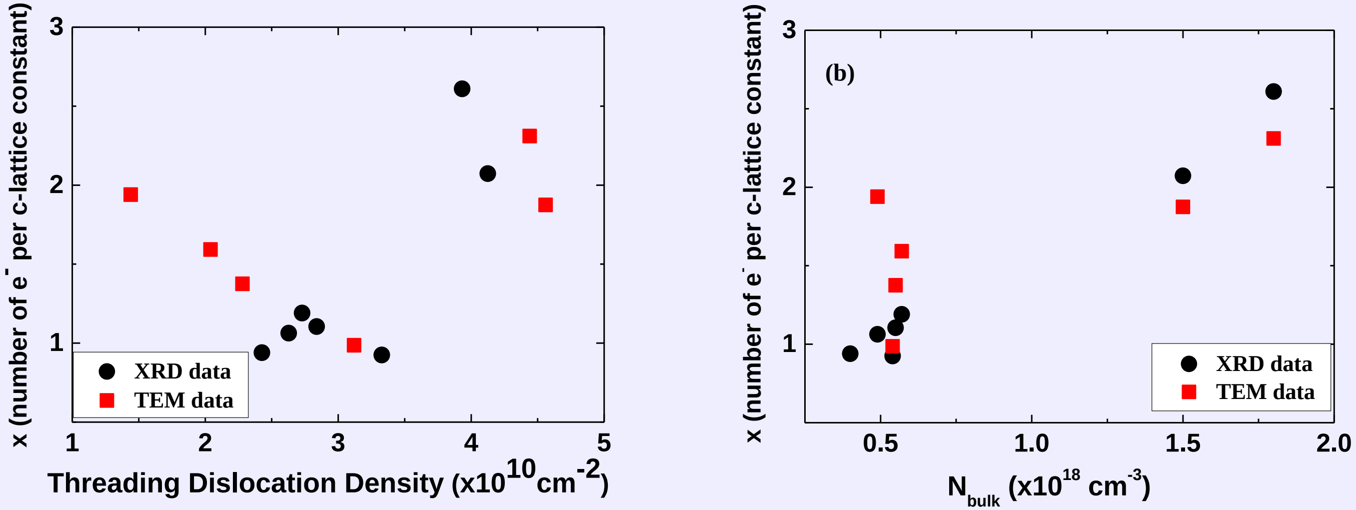

- ➢ **The number of electrons freed per c lattice constant length of dislocation line was estimated as** $x = \frac{N_{bulk}}{c \cdot TDD}$
- ➢ **Spreading of** x **values between 0.9 and 2.6** ***e/c***
- ➢ **Inconsistent with published mobility calculations. Assuming 1 e/c our mobility values would correspond to TDD~10^{9} cm^{-2} instead of ~10^{10} cm^{-2}**

- ➢ ***Bandgap ~0.623 eV determined from absorption edge spectrum (assuming constant refractive index)***
- ✓ **3.7 μm InN film, n$_{bulk}$ ≈ 3 x 10^{17} cm^{-3}, HRXRD N$_{TD}$ ≈ 6 x 10^{9} cm^{-2}**

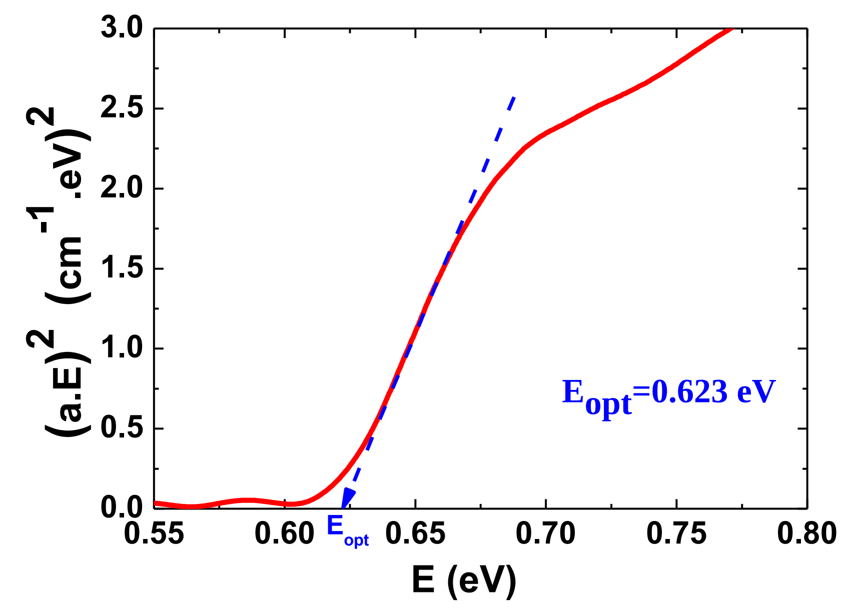

A. Adikimenakis et al., ECS J. Sol. St. Techn. 9, 015006 (2020)

InN drift velocity up to 10^8 cm^{-1}

- 775 nm InN-on-GaN (0001) film
- Resistors 8-µm long and 4-µm wide
- I-V measurements in pulsed mode (to avoid self-heating)
- v_d was calculated as v_d = I / qnhw, where q is the electron charge, n is the electron concentration and w is the resistor width

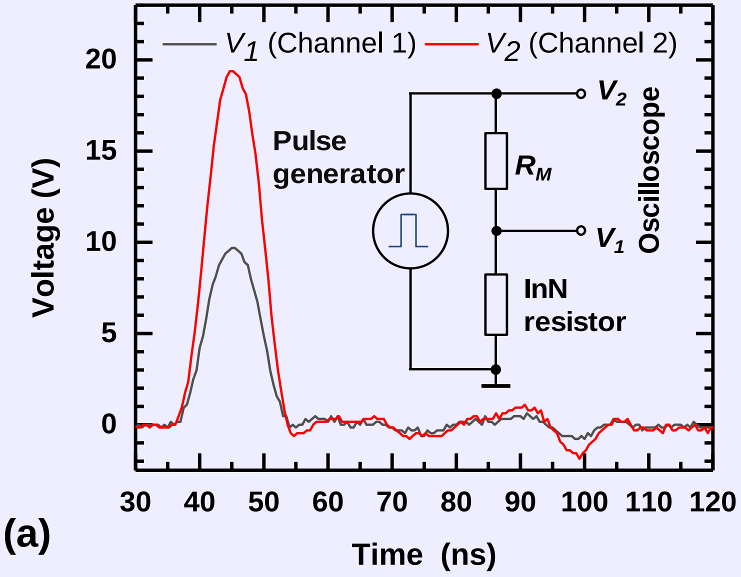

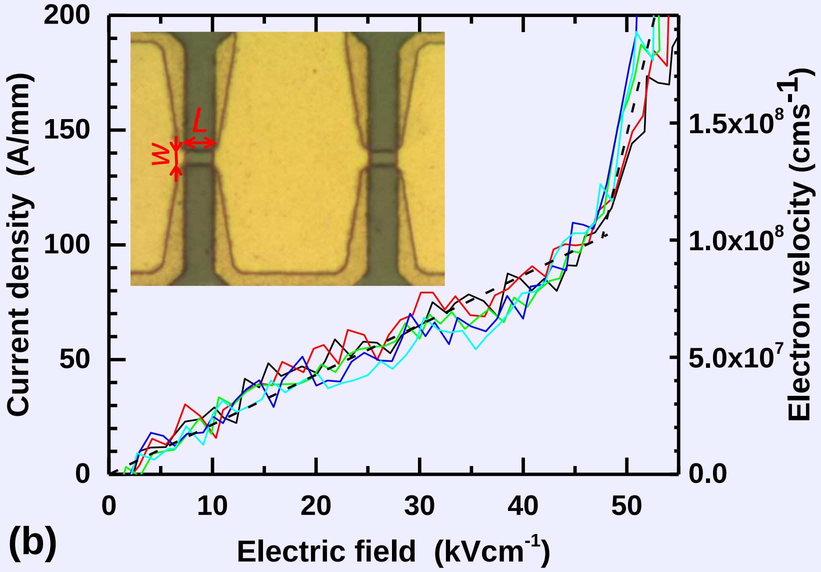

➢ Linear increase of the current and corresponding drift velocity values up to I ~ 100 A/mm at electric field ~ 48 kVcm^{-1}

➢ Electron drift velocity of ~1 × 10^8 cm s^{-1} at the electric field of ~ 48 kVcm^{-1} was determined

✓ Highest steady-state electron velocity ever measured in solid-state

J. Kuzmik et al, AIP Advances 11, 125325 (2021)

Increasing the InN-content in 1ML InN/GaN QWs

The 30% limit in x_{In} induced by N-rich surface reconstruction was extended to ~48% by In-rich MBE

Cross-sectional HRSTEM

T_d=550°C
L_{QW}=1 ML

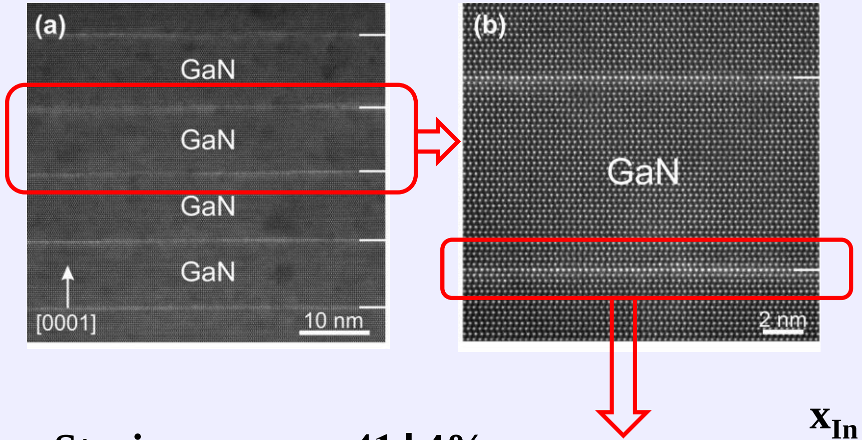

T_d=470°C, T_{GaN}=550°C
L_{QW}=2 ML

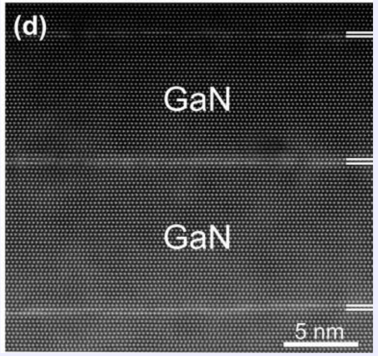

Strain map, x_{In}≈41±4%

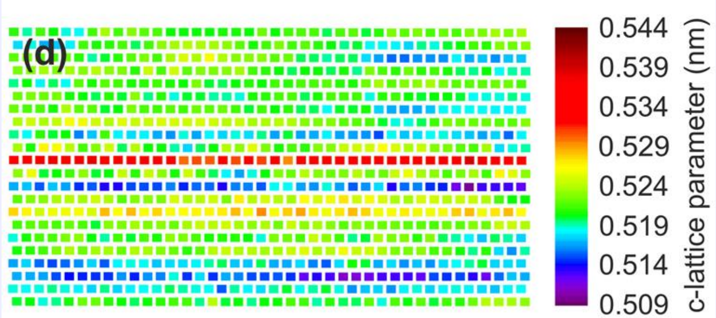

x_{In} from Z-contrast & multislice simulations

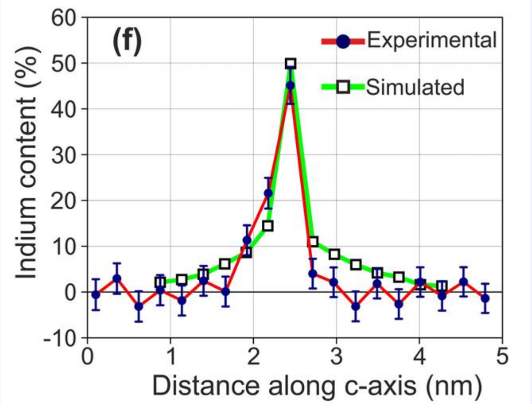

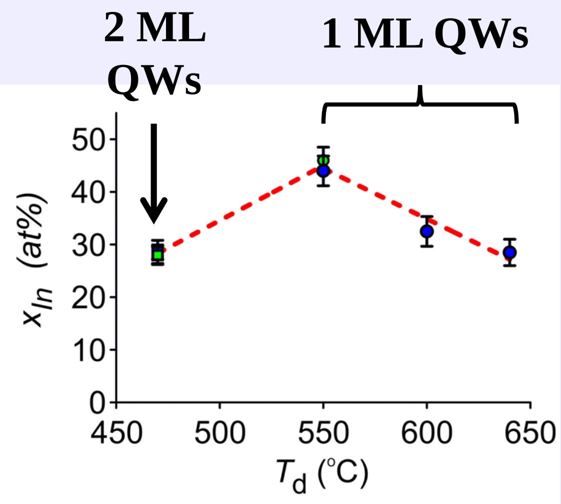

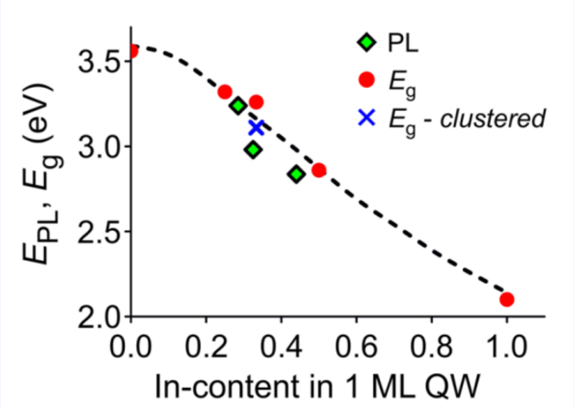

High T_d

- **Excellent overall crystal quality.**

Low Td

- **Low T_{GaN} detoriorates crystal quality (SFs, zb & wz phases)**
- **High T_{GaN} improves crystal quality.**

- **No ordering in InGaN QWs observed.**
- **In contents as high as ≈48% achieved**

A substitutional synthesis mechanism was proposed

I.G. Vasileiadis et al, Scientific Reports 11, 20606 (2021)

Spontaneous growth of GaN and InN nanowires

- *N-rich conditions lead to spontaneous GaN and InN NW growth on various substrates, such as Si*
- *NWs may grow self-organized or in selective areas of patterned substrates*

φ-scan of (11.4) GaN planes

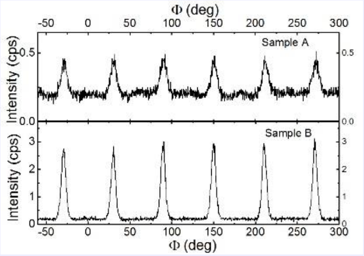

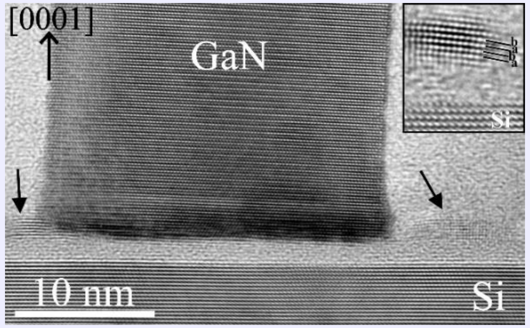

Silicon nitridation at 760º C for 20 min creates a smooth and homogenous Si_XN_Y substrate surface for uniform GaN NW nucleation

S. Eftychis et al, J. Cryst. Growth 442, 8 (2016)

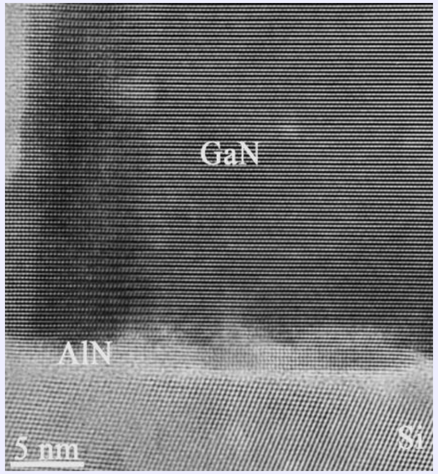

NW growth on Si without amorphous interfacial layer using 1.5nm AlN prelayer

S. Eftychis et al, J. Cryst. Growth 514, 89 (2019)

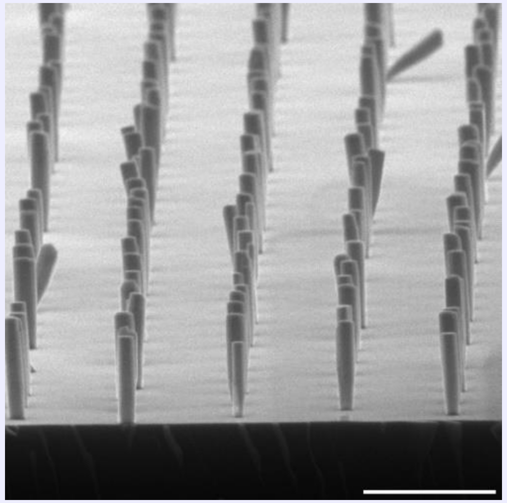

Selective Area Epitaxy on SiO_2-masked Si (111)

Mask holes with 1μm spacing were filled

J.E. Kruse et al, J. Appl. Phys. 119, 224305 (2016)

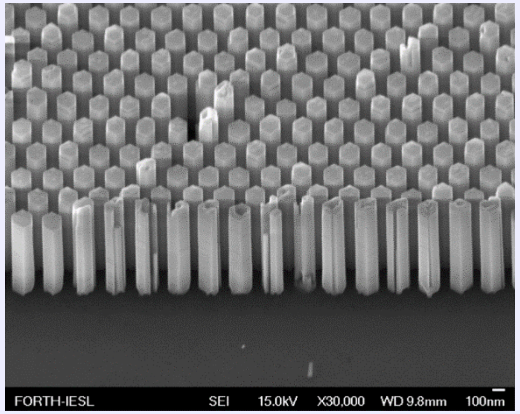

Selective Area Epitaxy on SiO_2-masked GaN

Mask holes with 0.25μm spacing were filled

Conclusions

- Molecular Beam Epitaxy of III-V semiconductors in Greece had to compete in the hard core of semiconductor technology that used to be a privilege of established institutions worldwide

- A wide range of III-V semiconductors are available at the MBE activity in Crete

- Fruitful collaborative work has been carried out within Greece in the past

- Hopefully, new opportunities of exploration will be found in the future

Acknowledgments

- **Financial support** of recent work by the Hellenic Foundation for Research and Innovation (H.F.R.I.) under the “First Call for H.F.R.I. Research Projects to support Faculty members and Researchers and the procurement of high-cost research equipment grant” (Project Number: HFRI-FM17-3173 “EPINEET”)

- **Scientific collaborations**

I have benefited from valuable collaborations with many scientists throughout all years. I will try to list the names of colleagues we have had long-term/impactful interactions

Aristotle University of Thessaloniki: Ph. Komninou, Th. Kehagias, G. Dimitrakopulos, J. Kioseglou, Th. Karakostas, E. Paloura, N. Katsikini, J. Arvanitidis, Ch. Lioutas, A. Delimitis and the late N. Flevaris and J. Stoemenos

University of Athens: M. Calamiotou and G. Papaioannou

NCSR Demokritos: P. Normand, P. Dimitrakis

NTUA: I. Raptis and D. Tsoukalas

University of Barcelona: F. Peiro and A. Cornet

SAS-IEE, Bratislava: Jan Kuzmik **EK MFA, Budapest:** Bela Pecz

FORTH & UoC: A numerous number of present or previous members of the Microelectronics Research Group. Especially the group’s founder Prof. Aris Christou and the late colleagues G. Halkias and P. Panayotatos

Thank you for your attention !

Questions are welcomed